Reduced-order state-space models of structures with imposed displacements and accelerations

G. Raze[a,*], C. Dumoulin[b], A. Deraemaeker[b]

[a] *Space Structures and Systems Laboratory, Aerospace and Mechanical Engineering Department, University of Liège Quartier Polytech 1 (B52/3), Allée de la Découverte 9, B-4000 Liège, Belgium*
[b] *Building Architecture and Town Planning (BATir), Université Libre de Bruxelles, 50 av Franklin Roosevelt CP 194/02, 1050 Brussels, Belgium*

Abstract

Generating reduced state-space models of base-excited structures is of great help in control engineering but is not straightforward to implement in practice, and this problem is addressed in this work. Methods to impose non-homogeneous boundary displacements or accelerations are reviewed, and a novel relative acceleration method is proposed to treat the case of imposed displacements. Various construction approaches for state-space models having prescribed displacements or accelerations as input and including a static correction term are then developed. The theoretical developments are eventually illustrated with structures of increasing complexity, namely, a bar, a beam, and a multi-story building model.

Keywords: Imposed displacement, Imposed acceleration, Base excitation, Reduced-order model, Craig-Bampton method, State-space model

Nomenclature

$\boldsymbol{\eta}$	Vector of modal coordinates
$\boldsymbol{\lambda}$	Vector of Lagrange multipliers
$\cdot_a$	Imposed acceleration
$\cdot_B$	Base (or boundary)
$\cdot_C$	Condensed
$\cdot_D$	Discarded
$\cdot_d$	Imposed displacement
$\cdot_f$	Imposed external forcing
$\cdot_I$	Internal
$\cdot_m$	Arbitrary method
$\cdot_P$	Prescribed
$\cdot_R$	Retained
$\cdot_r$	Relative
$\cdot_{CB}$	Craig-Bampton
$\cdot_{CNM}$	Component normal mode
$\cdot_{I,d}$	Internal dynamic
$\cdot_{I,s}$	Internal quasi-static
$\cdot_{MCB}$	Massless Craig-Bampton

*Corresponding author
Email address: g.raze@uliege.be (G. Raze)

$\cdot_{MN}$	MacNeal
$\cdot_{RAM}$	Relative acceleration method
$\cdot_{RA}$	Residual attachment mode
$\cdot_{RBM}$	Rigid body mode
$\cdot_{ref}$	Reference
$\cdot_{RMM}$	Relative motion method
$\mathbf{\Omega}$	Circular frequency matrix
$\mathbf{\Phi}$	Mode shape matrix
$\mathbf{B}$	Influence matrix
$\mathbf{C}$	Output matrix
$\mathbf{D}$	State-space feedthrough matrix
$\mathbf{f}$	Vector of generalized loadings
$\mathbf{I}$	Identity matrix
$\mathbf{K}$	Stiffness matrix
$\mathbf{M}$	Mass matrix
$\mathbf{q}$	Vector of generalized degrees of freedom
$\mathbf{T}$	Transformation matrix
$\mathbf{u}_f$	Vector of input generalized loadings
$\mathbf{u}_I$	Vector of transformed internal degrees of freedom
$\mathbf{Z}$	Modal damping ratio matrix
ω	Circular frequency
$\tilde{\cdot}$	Craig-Bampton matrix
$\bar{\cdot}$	Penalization matrix
$\breve{\cdot}$	Relative motion or acceleration method matrix
e	Error
k	Stiffness
m	Mass
q	Generalized degree of freedom
DAE	Differential-algebraic equation
DoF	Degree of freedom
FE	Finite element
FRF	Frequency response function
LMM	Large mass method
LSM	Large stiffness method
ODE	Ordinary differential equation
RAM	Relative acceleration method
RMM	Relative motion method
ROM	Reduced-order model
SDT	Structural Dynamics Toolbox

1. Introduction

Vibrations of structural systems are often analyzed through their response to external solicitations under the form of generalized loadings. In some cases, these loadings may come from support motion, e.g., when predicting the response of a building to seismic excitation [1], when assessing the performance of a precision mechatronics system in terms of transmissibility reduction [2], or when performing modal analysis [3, 4]. Imposing a motion on a given part of the structure amounts to solving partial differential equations with non-homogeneous boundary conditions [5]. Different methods can be used to model the imposition of the support motion for systems discretized with, e.g., the finite element (FE) method [6, 7].

Ideally, one has access to the full FE model of the structure, and imposing displacements and/or accelerations on some degrees of freedom (DoFs) is a relatively straightforward task with state-of-the-art methods [6]. In practice, reduced-order models (ROMs) are more often used to share structural models for economical and/or confidentiality reasons. In particular, the Craig-Bampton

reduction approach is very popular in research and industry [8, 7]. The purpose of this work is to address the problem of imposing boundary displacements and/or accelerations with ROMs. Furthermore, methods to build state-space models are reviewed and proposed. Such models are commonly used in various fields, such as the active control or system identification communities.

Base displacement, velocity and acceleration can directly and simultaneously be imposed to the structure [9]. A popular approach for imposing boundary conditions exactly (for undamped structures) is the relative motion method (RMM) [1]. This method assumes that the structural response can be expressed as the superposition of two contributions. The first one is a pseudo-static displacement given by the static response of the structure to its base displacement. The second one is the displacement relative to that pseudo-static displacement. This decomposition amounts to performing a coordinate transformation which decouples the stiffness interactions between constrained and free DoFs. Consequently, the contribution of the imposed displacements vanishes in the equations governing the free DoFs dynamics, thereby requiring only the knowledge of the imposed accelerations. Interestingly, a counterpart of this method for imposed displacements does not seem to exist in the literature. A probable reason for this is that the mass matrix is sometimes (approximated to be) diagonal, thereby featuring no inertial coupling between the constrained and free DoFs and allowing for a straightforward imposition of the boundary displacements.

Alternatively, penalization methods can be used to impose the boundary conditions [10]. The so-called large mass method (LMM) [1] and large stiffness method (LSM) [6, 10] artificially increase the mass and stiffness associated with DoFs on which accelerations and displacements are imposed, respectively. By doing so, the inertial and elastic forces resulting from the imposed accelerations and displacements, respectively, become dominant in the dynamical equilibrium. These imposed natural boundary conditions then force the structure into the corresponding essential boundary conditions. These methods are straightforward, versatile and easy to implement. The choice of the penalization magnitude results from a trade-off between accuracy and numerical conditioning. Paraskevopoulos et al [11] showed that these penalization methods are not suited for time integration schemes with conditional stability, unless they are simultaneously used with appropriate relative scaling. Liu et al [6] also evidenced structural frequency response functions (FRFs) that featured errors at low and high frequencies using the LSM and LMM, respectively. Finally, Qin and Li [12] discussed potential errors that may arise when damping is introduced into the model.

A last common type of method allowing for the imposition of displacements or acceleration consists in using Lagrange multipliers [7, 13, 10]. With this method, a set of p constraints is imposed through p additional algebraic equations to which are associated p unknown multipliers. Adding these equations to the original equations of motion results in a larger system of differential-algebraic equations (DAEs). In some cases, numerical conditioning can also be an issue with this method [14].

The rather large number of DoFs required for an accurate description of the structure dynamics and geometry leads to models of impractically large size. Classical model order reduction techniques using fixed [8] or free [15, 16, 17] interface modes are known to offer a practical solution to this issue. Among them, the Craig-Bampton method [8] is a standard in industry and is implemented in virtually any FE code. There exist reviews on such approaches, giving historical [18] and disciplinary [19] perspectives. Even after a first reduction, the number of interface DoFs may still be relatively large, requiring specialized interface reduction methods [20]. Some approaches also focus on specific frequency ranges. For instance, Kuhar and Stale proposed a dynamic reduction matrix depending on the frequency around which the reduction is performed [21]. Recently, Aumann

et al [22] presented an adaptive model order reduction approach to approximate the response of structures with frequency-dependent material properties.

ROMs are classically used for component mode synthesis or the analysis of forced responses, but very few works focused on the creation of reduced-order models specifically tailored for imposed displacements or accelerations. As presented in [7], the Craig-Bampton method is a reduced-order equivalent of the RMM, thereby naturally allowing for a straightforward imposition of boundary accelerations. It shall however be shown in this work that imposing boundary displacements with such ROMs is a less trivial problem.

The structural equations of motion are derived from Newton's or Lagrange's equations and are thus most of the time expressed through a set of second-order ordinary differential equations (ODEs). Alternatively, state-space models can be used as versatile and more general modeling tools. For instance, it is a popular choice in the active control community [23]. State-space models are also necessary to compute the complex modes of non-proportionally damped structures [24, 25]. Moreover, a series of state-of-the-art system identification techniques such as the subspace identification approach [26] result in a state-space model aiming to replicate the dynamics of the system under test. Converting the structural equations of motion to a state-space form with force inputs is rather straightforward (see, e.g., [7, 24]), but the inverse transformation is less trivial. This transformation is nonetheless important, because a formulation in second-order form is the cornerstone of classical structural dynamics, e.g., through modal analysis or specialized numerical integration schemes [7]. Such a transformation can also be used to perform model updating. This motivated a number of works to develop approaches allowing to retrieve a classical second-order representation [27], possibly under specific conditions on the inputs and outputs [28, 29] and constraints to impose physical consistency [30, 31]. Alternatively, methods were developed to directly work with these state-space models, allowing, e.g., to assemble models of different components that are physically connected via primal [32, 33] or dual [25] assembly procedures. Yet, very few works describe how to build state-space models taking imposed displacements or accelerations as input.

The purpose of this work is thus threefold. First, different methods to impose boundary accelerations and displacements are discussed and developed. They are either direct or use a coordinates transformation, penalization terms or Lagrange multipliers. In particular, a novel counterpart of the RMM method, called the relative acceleration method, is presented for imposed displacements. A second objective is to apply these methods to reduced-order models, with a specific emphasis on Craig-Bampton reduced-order models. Third, the resulting models are converted to equivalent state-space forms. The proposed methods are illustrated with numerical examples of increasing complexity, namely, a bar element, a cantilever beam, and a multi-story building.

2. An introductory example

Figure 1 schematizes a single-degree-of-freedom oscillator excited through its base motion q_B. The equation of motion using the absolute displacement of the oscillator q reads

$$m\ddot{q} + kq = kq_B, \tag{1}$$

where m and k are the mass and stiffness of the oscillator, respectively, and an upper dot denotes time differentiation. An alternate form is also frequently used with the relative displacement between the oscillator and its base given by

$$q_r = q - q_B. \tag{2}$$

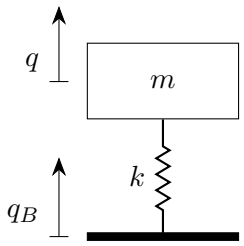

Figure 1: Base-excited single-degree-of-freedom oscillator.

Substituting q_r for q in Equation (1) using Equation (2), one gets

$$m\ddot{q}_r + kq_r = -m\ddot{q}_b. \tag{3}$$

Equations (1) and (3) show that using absolute and relative displacements is a natural way to impose base displacement and acceleration, respectively. These results shall be generalized to base-excited multiple-degree-of-freedom structures in the next section.

3. Imposing dynamic, non-homogeneous essential boundary conditions

The equations of motion of an undamped multiple-degree-of-freedom structure relate the generalized loadings $\mathbf{f}$ to the generalized DoFs $\mathbf{q}$ through the dynamical equations

$$\mathbf{M}\ddot{\mathbf{q}} + \mathbf{K}\mathbf{q} = \mathbf{f}, \tag{4}$$

where $\mathbf{M}$ and $\mathbf{K}$ are structural mass and stiffness matrices, respectively. The mass matrix is generally symmetric positive definite, while the stiffness matrix is generally positive semi-definite. It is assumed that the DoFs can be described by

$$\mathbf{q} = \mathbf{T}_B\mathbf{q}_B + \mathbf{T}_I\mathbf{q}_I \tag{5}$$

where subscript B (for "boundary") denotes the DoFs on which an acceleration or displacement is prescribed, whereas the remaining DoFs are indexed by the subscript I (for "internal"). As an example, if a the vector of generalized DoFs is reordered such that

$$\mathbf{q} = \begin{bmatrix} \mathbf{q}_B \\ \mathbf{q}_I \end{bmatrix}, \tag{6}$$

then these matrices are simply given by

$$\mathbf{T}_B = \begin{bmatrix} \mathbf{I} \\ \mathbf{0} \end{bmatrix}, \qquad \mathbf{T}_I = \begin{bmatrix} \mathbf{0} \\ \mathbf{I} \end{bmatrix}, \tag{7}$$

where matrices $\mathbf{I}$ and $\mathbf{0}$ are the identity and zero matrices, respectively, whose sizes are deduced from Equation (5). If the vector of generalized DoFs is not reordered according to Equation (6), these matrices are similar to those in Equation (7) with permuted rows. It should also be noted that Equation (5) is quite general and could also represent more sophisticated situations where kinematic constraints are enforced between the boundary DoFs.

A partition of the structural matrices after a congruent transformation given by

$$\begin{bmatrix}\mathbf{T}_B^T\\ \mathbf{T}_I^T\end{bmatrix}\mathbf{M}\begin{bmatrix}\mathbf{T}_B & \mathbf{T}_I\end{bmatrix}=\begin{bmatrix}\mathbf{M}_{BB} & \mathbf{M}_{BI}\\ \mathbf{M}_{IB} & \mathbf{M}_{II}\end{bmatrix},\qquad \begin{bmatrix}\mathbf{T}_B^T\\ \mathbf{T}_I^T\end{bmatrix}\mathbf{K}\begin{bmatrix}\mathbf{T}_B & \mathbf{T}_I\end{bmatrix}=\begin{bmatrix}\mathbf{K}_{BB} & \mathbf{K}_{BI}\\ \mathbf{K}_{IB} & \mathbf{K}_{II}\end{bmatrix}, \tag{8}$$

is considered. With this partition, Equation (4) can equivalently be written

$$\begin{bmatrix}\mathbf{M}_{BB} & \mathbf{M}_{BI}\\ \mathbf{M}_{IB} & \mathbf{M}_{II}\end{bmatrix}\begin{bmatrix}\ddot{\mathbf{q}}_B\\ \ddot{\mathbf{q}}_I\end{bmatrix}+\begin{bmatrix}\mathbf{K}_{BB} & \mathbf{K}_{BI}\\ \mathbf{K}_{IB} & \mathbf{K}_{II}\end{bmatrix}\begin{bmatrix}\mathbf{q}_B\\ \mathbf{q}_I\end{bmatrix}=\begin{bmatrix}\mathbf{f}_B\\ \mathbf{f}_I\end{bmatrix}, \tag{9}$$

with

$$\begin{bmatrix}\mathbf{T}_B^T\\ \mathbf{T}_I^T\end{bmatrix}\mathbf{f}=\begin{bmatrix}\mathbf{f}_B\\ \mathbf{f}_I\end{bmatrix}. \tag{10}$$

The imposition of acceleration and displacement on the boundary DoFs can be performed with a direct approach [9]. The acceleration and displacement of the boundary DoFs are prescribed by $\ddot{\mathbf{q}}_B = \ddot{\mathbf{q}}_P$ and $\mathbf{q}_B = \mathbf{q}_P$, respectively, where subscript P stands for prescribed. The second set of equations in Equation (9) can then be rewritten

$$\mathbf{M}_{II}\ddot{\mathbf{q}}_I + \mathbf{K}_{II}\mathbf{q}_I = \mathbf{f}_I - \mathbf{M}_{IB}\ddot{\mathbf{q}}_P - \mathbf{K}_{IB}\mathbf{q}_P, \tag{11}$$

where $-\mathbf{M}_{IB}\ddot{\mathbf{q}}_P$ and $-\mathbf{K}_{IB}\mathbf{q}_P$ are inertia and restoring forces resulting from the imposed accelerations $\ddot{\mathbf{q}}_P$ and displacements $\mathbf{q}_P$, respectively. An inconvenient feature of Equation (11) is that it requires the simultaneous knowledge of (kinematically consistent) boundary displacement and acceleration as inputs to the system. Generally, only one kind of signal is known and the other one has to be obtained through numerical integration or differentiation. This also requires more data and computations, and can lead to physically inconsistent results if the imposed acceleration and displacement are not consistent themselves (e.g., due to an error of the user).

Various techniques aiming to evaluate the structural response knowing only one type of signal were proposed in the literature. They are reviewed or developed in the sequel and are separated into methods prescribing accelerations or displacements. The generalization to hybrid methods imposing accelerations on some boundary DoFs and displacements on the rest of them can be obtained without difficulty through a more refined partitioning of the boundary DoFs $\mathbf{q}_B$.

3.1. Imposed acceleration

Techniques that work with imposed accelerations, i.e., aiming to enforce $\ddot{\mathbf{q}}_B = \ddot{\mathbf{q}}_P$ without requiring the explicit knowledge of $\mathbf{q}_P$, are reviewed first.

3.1.1. Direct method

The requirement for simultaneous knowledge of the imposed displacement and acceleration raised by the direct method in Equation (11) can be relaxed at the expense of the symmetry of the structural matrices. Indeed, using only the prescribed acceleration $\ddot{\mathbf{q}}_P$, the equations of motion can be rewritten as

$$\begin{bmatrix}\mathbf{I} & \mathbf{0}\\ \mathbf{M}_{IB} & \mathbf{M}_{II}\end{bmatrix}\begin{bmatrix}\ddot{\mathbf{q}}_B\\ \ddot{\mathbf{q}}_I\end{bmatrix}+\begin{bmatrix}\mathbf{0} & \mathbf{0}\\ \mathbf{K}_{IB} & \mathbf{K}_{II}\end{bmatrix}\begin{bmatrix}\mathbf{q}_B\\ \mathbf{q}_I\end{bmatrix}=\begin{bmatrix}\ddot{\mathbf{q}}_P\\ \mathbf{f}_I\end{bmatrix}. \tag{12}$$

We note that the block-upper triangular structure of the mass matrix could potentially compensate for its lack of symmetry if efficiently exploited. For instance, using block matrix inversion formulas [34], inverting (or factoring) this matrix would only require knowing the inverse (or factorization) of $\mathbf{M}_{II}$. Similar considerations would apply for the dynamic stiffness matrix $\mathbf{K} - \omega^2\mathbf{M}$ for frequency-domain analysis since it would have the same structure.

3.1.2. Relative motion method

In the RMM [1], the internal DoFs are expressed as the superposition of a quasi-static motion due to the displacement of the boundary DoFs given by

$$\mathbf{q}_{I,s} = -\mathbf{K}_{II}^{-1}\mathbf{K}_{IB}\mathbf{q}_B \tag{13}$$

and a dynamic, relative motion given by

$$\mathbf{q}_{I,d} = \mathbf{T}_{I,d}\mathbf{u}_I. \tag{14}$$

It is assumed here for generality that $\mathbf{T}_{I,d}$ is a generic, full-rank matrix, and $\mathbf{u}_I$ are the coordinates corresponding to $\mathbf{q}_{I,d}$ before transformation by $\mathbf{T}_{I,d}$. In most cases, $\mathbf{T}_{I,d}$ is either the identity matrix (if no reduction is performed), or is given by the mode shapes of the structure with fixed boundary DoFs (see [1, 7] or Section 4.1).

The matrix $-\mathbf{K}_{II}^{-1}\mathbf{K}_{IB}$ describes the so-called constraint modes. Its columns correspond to the static deflection undergone by the internal DoFs when a unit displacement is imposed on the corresponding boundary DoF, with every other boundary DoF set to zero. Interestingly, these constraint modes correspond to the dynamic transformation matrix with stiffness coupling proposed in [21] and evaluated at zero frequency.

The superposition $\mathbf{q}_I = \mathbf{q}_{I,s} + \mathbf{q}_{I,d}$ can be expressed through the coordinate change

$$\begin{bmatrix}\mathbf{q}_B\\ \mathbf{q}_I\end{bmatrix} = \mathbf{T}_{RMM}\begin{bmatrix}\mathbf{q}_B\\ \mathbf{u}_I\end{bmatrix} = \begin{bmatrix}\mathbf{I} & \mathbf{0}\\ -\mathbf{K}_{II}^{-1}\mathbf{K}_{IB} & \mathbf{T}_{I,d}\end{bmatrix}\begin{bmatrix}\mathbf{q}_B\\ \mathbf{u}_I\end{bmatrix}. \tag{15}$$

Applying a congruent transformation with the matrix $\mathbf{T}_{RMM}$ to the structural matrices in Equation (9) yields

$$\begin{bmatrix}\breve{\mathbf{M}}_{BB} & \breve{\mathbf{M}}_{BI}\\ \breve{\mathbf{M}}_{IB} & \mathbf{T}_{I,d}^T\mathbf{M}_{II}\mathbf{T}_{I,d}\end{bmatrix}\begin{bmatrix}\ddot{\mathbf{q}}_B\\ \ddot{\mathbf{u}}_I\end{bmatrix} + \begin{bmatrix}\mathbf{K}_{BB} - \mathbf{K}_{BI}\mathbf{K}_{II}^{-1}\mathbf{K}_{IB} & \mathbf{0}\\ \mathbf{0} & \mathbf{T}_{I,d}^T\mathbf{K}_{II}\mathbf{T}_{I,d}\end{bmatrix}\begin{bmatrix}\mathbf{q}_B\\ \mathbf{u}_I\end{bmatrix} = \begin{bmatrix}\mathbf{f}_B - \mathbf{K}_{BI}\mathbf{K}_{II}^{-1}\mathbf{f}_I\\ \mathbf{T}_{I,d}^T\mathbf{f}_I\end{bmatrix} \tag{16}$$

where

$$\breve{\mathbf{M}}_{BB} = \mathbf{M}_{BB} - \mathbf{M}_{BI}\mathbf{K}_{II}^{-1}\mathbf{K}_{IB} - \mathbf{K}_{BI}\mathbf{K}_{II}^{-1}\mathbf{M}_{IB} + \mathbf{K}_{BI}\mathbf{K}_{II}^{-1}\mathbf{M}_{II}\mathbf{K}_{II}^{-1}\mathbf{K}_{IB} \tag{17}$$

and

$$\breve{\mathbf{M}}_{BI} = \mathbf{M}_{BI}\mathbf{T}_{I,d} - \mathbf{K}_{BI}\mathbf{K}_{II}^{-1}\mathbf{M}_{II}\mathbf{T}_{I,d} = \breve{\mathbf{M}}_{IB}^T. \tag{18}$$

The block diagonal structure of the stiffness matrix featured in Equation (16) indicates that the transformation allows for a static decoupling between the boundary and internal DoFs. The equations of motion with imposed boundary acceleration thus reduce to

$$\mathbf{T}_{I,d}^T\mathbf{M}_{II}\mathbf{T}_{I,d}\ddot{\mathbf{u}}_I + \mathbf{T}_{I,d}^T\mathbf{K}_{II}\mathbf{T}_{I,d}\mathbf{u}_I = \mathbf{T}_{I,d}^T\mathbf{f}_I - \breve{\mathbf{M}}_{IB}\ddot{\mathbf{q}}_P. \tag{19}$$

An important subcase of the RMM happens when a rigid interface motion is imposed. In such a case, the prescribed acceleration can be written

$$\ddot{\mathbf{q}}_P = \mathbf{\Phi}_{RBM,B}\ddot{\boldsymbol{\eta}}_{RBM,P}, \tag{20}$$

where $\mathbf{\Phi}_{RBM}$ is a matrix of rigid body modes ($\mathbf{\Phi}_{RBM,B}$ being its restriction to the boundary DoFs), and $\ddot{\boldsymbol{\eta}}_{RBM,P}$ is a vector describing the prescribed global motion of the base in terms of these rigid body modes (combined translation and rotation).

Now, since by definition of the rigid body modes

$$\mathbf{K}\boldsymbol{\Phi}_{RBM} = \begin{bmatrix} \mathbf{K}_{BB} & \mathbf{K}_{BI} \\ \mathbf{K}_{IB} & \mathbf{K}_{II} \end{bmatrix} \begin{bmatrix} \boldsymbol{\Phi}_{RBM,B} \\ \boldsymbol{\Phi}_{RBM,I} \end{bmatrix} = \mathbf{0}. \tag{21}$$

Equations (13), (20) and (21) then indicate that

$$\ddot{\mathbf{q}}_{I,s} = -\mathbf{K}_{II}^{-1}\mathbf{K}_{IB}\boldsymbol{\Phi}_{RBM,B}\ddot{\boldsymbol{\eta}}_{RBM,P} = \boldsymbol{\Phi}_{RBM,I}\ddot{\boldsymbol{\eta}}_{RBM,P}, \tag{22}$$

i.e., the constraint modes are the rigid body modes in this case. Choosing now $\mathbf{T}_{I,d} = \mathbf{I}$, the superposition $\mathbf{q}_I = \mathbf{q}_{I,s} + \mathbf{q}_{I,d}$ indicates that $\mathbf{q}_{I,d}$ (or $\mathbf{u}_I$) can be interpreted as the motion of the internal DoFs relative to the base. Equation (19) then becomes

$$\mathbf{M}_{II}\ddot{\mathbf{q}}_{I,d} + \mathbf{K}_{II}\mathbf{q}_{I,d} = \mathbf{f}_I - \left(\mathbf{M}_{IB}\boldsymbol{\Phi}_{RBM,B} + \mathbf{M}_{II}\boldsymbol{\Phi}_{RBM,I}\right)\ddot{\boldsymbol{\eta}}_{RBM,P}. \tag{23}$$

Such a model can easily be built from the full finite element model. Consequently, writing the equations of motion in terms of displacements relative to the base motion is a popular approach. Equation (23) can be seen as a generalization of Equation (3), and can only be used for rigid support motion.

3.1.3. Large mass method

The LMM [1] is a penalization approach. Introducing an invertible penalization matrix $\overline{\mathbf{M}}_{BB}$ that acts as fictitious mass added to the boundary DoFs, Equation (9) is changed to

$$\begin{bmatrix} \mathbf{M}_{BB} + \overline{\mathbf{M}}_{BB} & \mathbf{M}_{BI} \\ \mathbf{M}_{IB} & \mathbf{M}_{II} \end{bmatrix} \begin{bmatrix} \ddot{\mathbf{q}}_B \\ \ddot{\mathbf{q}}_I \end{bmatrix} + \begin{bmatrix} \mathbf{K}_{BB} & \mathbf{K}_{BI} \\ \mathbf{K}_{IB} & \mathbf{K}_{II} \end{bmatrix} \begin{bmatrix} \mathbf{q}_B \\ \mathbf{q}_I \end{bmatrix} = \begin{bmatrix} \overline{\mathbf{M}}_{BB}\ddot{\mathbf{q}}_P \\ \mathbf{f}_I \end{bmatrix}. \tag{24}$$

As $\overline{\mathbf{M}}_{BB}$ becomes large compared to the other involved terms, the dynamic equations for the boundary DoFs tend to

$$\overline{\mathbf{M}}_{BB}\ddot{\mathbf{q}}_B \approx \overline{\mathbf{M}}_{BB}\ddot{\mathbf{q}}_P, \tag{25}$$

i.e., $\ddot{\mathbf{q}}_B \approx \ddot{\mathbf{q}}_P$.

3.1.4. Lagrange multipliers method

Lagrange multipliers are commonly used as indirect means to impose boundary conditions. Introducing the vector of Lagrange multipliers[1] $\ddot{\boldsymbol{\lambda}}$, Equation (9) is augmented as

$$\begin{bmatrix} \mathbf{M}_{BB} & \mathbf{M}_{BI} & \mathbf{I} \\ \mathbf{M}_{IB} & \mathbf{M}_{II} & \mathbf{0} \\ \mathbf{I} & \mathbf{0} & \mathbf{0} \end{bmatrix} \begin{bmatrix} \ddot{\mathbf{q}}_B \\ \ddot{\mathbf{q}}_I \\ \ddot{\boldsymbol{\lambda}} \end{bmatrix} + \begin{bmatrix} \mathbf{K}_{BB} & \mathbf{K}_{BI} & \mathbf{0} \\ \mathbf{K}_{IB} & \mathbf{K}_{II} & \mathbf{0} \\ \mathbf{0} & \mathbf{0} & \mathbf{0} \end{bmatrix} \begin{bmatrix} \mathbf{q}_B \\ \mathbf{q}_I \\ \boldsymbol{\lambda} \end{bmatrix} = \begin{bmatrix} \mathbf{f}_B \\ \mathbf{f}_I \\ \ddot{\mathbf{q}}_P \end{bmatrix}. \tag{26}$$

The last set of equations enforces $\ddot{\mathbf{q}}_B = \ddot{\mathbf{q}}_P$, whereas in the first set of equations the Lagrange multipliers $\ddot{\boldsymbol{\lambda}}$ can be interpreted as constraint forces necessary to impose this motion.

3.2. Imposed displacement

Methods aiming to enforce prescribed displacements on the boundary DoFs as $\mathbf{q}_B = \mathbf{q}_P$ without knowing $\ddot{\mathbf{q}}_P$ explicitly are now reviewed.

[1] The double time derivation is not strictly necessary but is used here for notational consistency.

3.2.1. Direct method

The counterpart of Equation (12) for a prescribed displacement $\mathbf{q}_P$,

$$\begin{bmatrix} \mathbf{0} & \mathbf{0} \\ \mathbf{M}_{IB} & \mathbf{M}_{II} \end{bmatrix} \begin{bmatrix} \ddot{\mathbf{q}}_B \\ \ddot{\mathbf{q}}_I \end{bmatrix} + \begin{bmatrix} \mathbf{I} & \mathbf{0} \\ \mathbf{K}_{IB} & \mathbf{K}_{II} \end{bmatrix} \begin{bmatrix} \mathbf{q}_B \\ \mathbf{q}_I \end{bmatrix} = \begin{bmatrix} \mathbf{q}_P \\ \mathbf{f}_I \end{bmatrix}, \tag{27}$$

is a set of DAEs. This is an issue for time simulations, and state-space models construction, as shall be discussed in Section 5. However, frequency-domain calculations are not hampered by the fact that the governing equations are DAEs and not ODEs, because they cast the differential equations to algebraic ones, thereby resulting in a set of only algebraic equations.

It should nonetheless be noted that the mass matrix of a full finite element model given in Equation (4) is frequently close to be diagonal. In this case, the inertia coupling term $\mathbf{M}_{IB}$ can be neglected in Equation (11), so that

$$\mathbf{M}_{II}\ddot{\mathbf{q}}_I + \mathbf{K}_{II}\mathbf{q}_I = \mathbf{f}_I - \mathbf{K}_{IB}\mathbf{q}_P, \tag{28}$$

which then only requires the prescribed displacements. When the mass matrix is not close to be diagonal however, such as can be the case for reduced-order models (see Section 4.3), doing so may result in substantial error.

3.2.2. Relative acceleration method

Similarly to the RMM, a relative acceleration method (RAM) is proposed herein, expressing the internal DoFs motion as the sum of an acceleration due to the boundary DoFs and an acceleration relative to this motion. The former is given by

$$\ddot{\mathbf{q}}_{I,a} = -\mathbf{M}_{II}^{-1}\mathbf{M}_{IB}\ddot{\mathbf{q}}_B. \tag{29}$$

The columns of the matrix $-\mathbf{M}_{II}^{-1}\mathbf{M}_{IB}$ can (rather abstractly) be interpreted as the acceleration that would be undergone by the internal DoFs if a unit-amplitude acceleration was imposed at infinite frequency on the boundary DoF corresponding to the considered column, with every other boundary DoF set to zero. This can be deduced from Equation (11), where $\mathbf{f}_I = \mathbf{0}$ and the contribution of stiffness forces becomes negligible compared to the inertia forces due to the infinitely high frequency. These deformations are called inertial modes in the sequel. It should be emphasized that these modes pertain to the *model* of the structure rather than the structure itself, because the former is not expected to be a good representative of the latter at high frequencies. These modes thus do not bear a physical sense unless the discretization is infinite. Yet, this method does not introduce additional approximations with respect to the initial model. Interestingly, the inertial modes correspond to the limit of the dynamic transformation matrix with inertial coupling proposed in [21] when the frequency tends to infinity.

Using a generic, full-rank transformation matrix $\mathbf{T}_{I,d}$ for the internal DoFs, the superposition can thus be expressed by

$$\begin{bmatrix} \mathbf{q}_B \\ \mathbf{q}_I \end{bmatrix} = \mathbf{T}_{RAM} \begin{bmatrix} \mathbf{q}_B \\ \mathbf{u}_I \end{bmatrix} = \begin{bmatrix} \mathbf{I} & \mathbf{0} \\ -\mathbf{M}_{II}^{-1}\mathbf{M}_{IB} & \mathbf{T}_{I,d} \end{bmatrix} \begin{bmatrix} \mathbf{q}_B \\ \mathbf{u}_I \end{bmatrix}. \tag{30}$$

Applying this transformation to Equation (9) yields

$$\begin{bmatrix} \mathbf{M}_{BB} - \mathbf{M}_{BI}\mathbf{M}_{II}^{-1}\mathbf{M}_{IB} & \mathbf{0} \\ \mathbf{0} & \mathbf{T}_{I,d}^T\mathbf{M}_{II}\mathbf{T}_{I,d} \end{bmatrix} \begin{bmatrix} \ddot{\mathbf{q}}_B \\ \ddot{\mathbf{u}}_I \end{bmatrix} + \begin{bmatrix} \breve{\mathbf{K}}_{BB} & \breve{\mathbf{K}}_{BI} \\ \breve{\mathbf{K}}_{IB} & \mathbf{T}_{I,d}^T\mathbf{K}_{II}\mathbf{T}_{I,d} \end{bmatrix} \begin{bmatrix} \mathbf{q}_B \\ \mathbf{u}_I \end{bmatrix} = \begin{bmatrix} \mathbf{f}_B - \mathbf{M}_{BI}\mathbf{M}_{II}^{-1}\mathbf{f}_I \\ \mathbf{T}_{I,d}^T\mathbf{f}_I \end{bmatrix}, \tag{31}$$

where

$$\breve{\mathbf{K}}_{BB} = \mathbf{K}_{BB} - \mathbf{K}_{BI}\mathbf{M}_{II}^{-1}\mathbf{M}_{IB} - \mathbf{M}_{BI}\mathbf{M}_{II}^{-1}\mathbf{K}_{IB} + \mathbf{M}_{BI}\mathbf{M}_{II}^{-1}\mathbf{K}_{II}\mathbf{M}_{II}^{-1}\mathbf{M}_{IB} \tag{32}$$

and

$$\breve{\mathbf{K}}_{BI} = \mathbf{K}_{BI}\mathbf{T}_{I,d} - \mathbf{M}_{BI}\mathbf{M}_{II}^{-1}\mathbf{K}_{II}\mathbf{T}_{I,d} = \breve{\mathbf{K}}_{IB}^{T}. \tag{33}$$

Just like the RMM allows for static decoupling between the internal and boundary DoFs, the RAM allows for inertial decoupling. From Equation (31), the equations of motion with imposed boundary displacement thus reduce to

$$\mathbf{T}_{I,d}^{T}\mathbf{M}_{II}\mathbf{T}_{I,d}\ddot{\mathbf{u}}_I + \mathbf{T}_{I,d}^{T}\mathbf{K}_{II}\mathbf{T}_{I,d}\mathbf{u}_I = \mathbf{T}_{I,d}^{T}\mathbf{f}_I - \breve{\mathbf{K}}_{IB}\mathbf{q}_P. \tag{34}$$

When the inertia coupling term $\mathbf{M}_{IB}$ is zero or negligible and when one chooses $\mathbf{T}_{I,d} = \mathbf{I}$, Equation (30) shows that a natural choice for imposed displacements is to keep absolute displacements as generalized DoFs, as discussed in Section 3.2.1. This can also be seen as a generalization of the approach used in Equation (1).

3.2.3. Large stiffness method

Similarly to the LMM, the LSM uses a penalization term under the form of a large, invertible stiffness matrix $\overline{\mathbf{K}}_{BB}$ [6, 10] and changes Equation (9) to

$$\begin{bmatrix}\mathbf{M}_{BB} & \mathbf{M}_{BI}\\ \mathbf{M}_{IB} & \mathbf{M}_{II}\end{bmatrix}\begin{bmatrix}\ddot{\mathbf{q}}_B\\ \ddot{\mathbf{q}}_I\end{bmatrix} + \begin{bmatrix}\mathbf{K}_{BB} + \overline{\mathbf{K}}_{BB} & \mathbf{K}_{BI}\\ \mathbf{K}_{IB} & \mathbf{K}_{II}\end{bmatrix}\begin{bmatrix}\mathbf{q}_B\\ \mathbf{q}_I\end{bmatrix} = \begin{bmatrix}\overline{\mathbf{K}}_{BB}\mathbf{q}_P\\ \mathbf{f}_I\end{bmatrix}. \tag{35}$$

As this penalization term grows larger, the dynamic equilibrium of the boundary DoFs tends to

$$\overline{\mathbf{K}}_{BB}\mathbf{q}_B \approx \overline{\mathbf{K}}_{BB}\mathbf{q}_P, \tag{36}$$

i.e.,

$$\mathbf{q}_B \approx \mathbf{q}_P, \tag{37}$$

without directly affecting the dynamics of the internal DoFs.

3.2.4. Lagrange multipliers method

Finally, the method of Lagrange multipliers can be used to impose boundary displacements. The vector of Lagrange multipliers $\boldsymbol{\lambda}$ (which can once again be interpreted as the force necessary to impose the desired boundary displacement) is incorporated into the equations of motion to enforce $\mathbf{q}_B = \mathbf{q}_P$ by

$$\begin{bmatrix}\mathbf{M}_{BB} & \mathbf{M}_{BI} & \mathbf{0}\\ \mathbf{M}_{IB} & \mathbf{M}_{II} & \mathbf{0}\\ \mathbf{0} & \mathbf{0} & \mathbf{0}\end{bmatrix}\begin{bmatrix}\ddot{\mathbf{q}}_B\\ \ddot{\mathbf{q}}_I\\ \ddot{\boldsymbol{\lambda}}\end{bmatrix} + \begin{bmatrix}\mathbf{K}_{BB} & \mathbf{K}_{BI} & \mathbf{I}\\ \mathbf{K}_{IB} & \mathbf{K}_{II} & \mathbf{0}\\ \mathbf{I} & \mathbf{0} & \mathbf{0}\end{bmatrix}\begin{bmatrix}\mathbf{q}_B\\ \mathbf{q}_I\\ \boldsymbol{\lambda}\end{bmatrix} = \begin{bmatrix}\mathbf{f}_B\\ \mathbf{f}_I\\ \mathbf{q}_P\end{bmatrix}. \tag{38}$$

We note that, similarly to the direct method and unlike Equation (26), Equation (38) represents a set of DAEs. Again, these DAEs may require special numerical treatment for time simulations, and prevent the construction of a state-space model, but do not cause any difficulty for frequency-domain calculations.

3.3. Qualitative comparison of the different approaches

This section presented various approaches to impose boundary displacements and/or accelerations. To conclude it, these methods are briefly compared qualitatively.

The direct approach is the most straightforward one but requires the simultaneous imposition of displacement and acceleration in general. An alternative where only the prescribed acceleration is required was proposed, but this destroys the symmetry of the structural matrices. It does not seem possible to find a counterpart prescribing boundary displacement only and yielding ODEs, except in the case where the mass matrix is (approximated to be) diagonal.

The RMM and RAM require more computations beforehand, but result in a model with a minimum number of unknowns, similarly to the direct approach. When a rigid base acceleration is prescribed, the RMM simplifies to a formulation that uses displacements relative to the base as DoFs. The RAM simplifies to an approach where absolute displacements are used when the mass matrix is diagonal (and approaches it when the matrix is close to diagonal). These two approaches thus naturally generalize the single-degree-of-freedom case presented in Section 2.

Penalization methods are fairly simple, but are inexact. This issue can be mitigated by choosing a sufficiently large penalization term, as long as the latter does not result in numerical ill conditioning. Choosing an adequate penalization term is thus a trial and error procedure in general.

Using Lagrange multipliers allows for an exact imposition of the boundary conditions and for the evaluation of the external forces needed to impose these conditions. However, this results in a system with a larger number of unknowns. Furthermore, the mass (stiffness) matrix loses its definiteness and the stiffness (mass) matrix is necessarily singular when imposing accelerations (displacements).

4. Model order reduction

Reduced-order models are commonly used as they allow for an accurate description of the structural dynamics with a reduced number of unknowns. Moreover, a structural system as a whole generally results from the assembly of multiple substructures designed by different teams, possibly from different companies. For economy and/or confidentiality reasons, reduced-order models of these substructures are shared among the teams. These substructures can then be reassembled to evaluate the dynamical behavior of the whole system. Such an approach is called dynamic substructuring [7, 35].

Among the various proposed approaches, the Craig-Bampton reduction is the most popular one [8], which is why the emphasis is put on this technique in this work. A brief account on other approaches is also given at the end of this section.

To perform model order reduction, Equation (4) is partitioned as

$$\begin{bmatrix} \mathbf{M}_{RR} & \mathbf{M}_{RC} \\ \mathbf{M}_{CR} & \mathbf{M}_{CC} \end{bmatrix} \begin{bmatrix} \ddot{\mathbf{q}}_R \\ \ddot{\mathbf{q}}_C \end{bmatrix} + \begin{bmatrix} \mathbf{K}_{RR} & \mathbf{K}_{RC} \\ \mathbf{K}_{CR} & \mathbf{K}_{CC} \end{bmatrix} \begin{bmatrix} \mathbf{q}_R \\ \mathbf{q}_C \end{bmatrix} = \begin{bmatrix} \mathbf{f}_R \\ \mathbf{f}_C \end{bmatrix}, \tag{39}$$

where subscripts R and C stand for retained and condensed, respectively. The retained DoFs should include the boundary DoFs defined in Section 3, but can also include other DoFs.

4.1. Craig-Bampton reduction

The Craig-Bampton method [8] is based on the superposition of constraint modes and fixed-interface modes, also called component normal modes. The latter are the solution of the generalized

eigenvalue problem

$$\mathbf{K}_{CC}\mathbf{\Phi}_{CNM} = \mathbf{M}_{CC}\mathbf{\Phi}_{CNM}\mathbf{\Omega}^2_{CNM}, \tag{40}$$

where $\mathbf{\Omega}_{CNM}$ is a diagonal matrix containing the mode frequencies, $\mathbf{\Phi}_{CNM}$ is a mode shape matrix, and subscript CNM stands for component normal modes. The mode shapes are usually mass-normalized, i.e.,

$$\mathbf{\Phi}^T_{CNM}\mathbf{M}_{CC}\mathbf{\Phi}_{CNM} = \mathbf{I}, \qquad \mathbf{\Phi}^T_{CNM}\mathbf{K}_{CC}\mathbf{\Phi}_{CNM} = \mathbf{\Omega}^2_{CNM}. \tag{41}$$

The Craig-Bampton reduction is performed by keeping a reduced subset of fixed-interface modes (i.e., $\mathbf{\Phi}_{CNM}$ has less columns than rows). This defines a reduction matrix by

$$\mathbf{q} \approx \begin{bmatrix} \mathbf{I} & \mathbf{0} \\ -\mathbf{K}^{-1}_{CC}\mathbf{K}_{CR} & \mathbf{\Phi}_{CNM} \end{bmatrix} \begin{bmatrix} \mathbf{q}_R \\ \boldsymbol{\eta}_C \end{bmatrix} = \mathbf{T}_{CB} \begin{bmatrix} \mathbf{q}_R \\ \boldsymbol{\eta}_C \end{bmatrix}, \tag{42}$$

where $\boldsymbol{\eta}_C$ is the vector of modal coordinates associated with the retained fixed-interface modes, and subscript CB stands for Craig-Bampton.

The Craig-Bampton reduced stiffness and mass matrices are respectively obtained as

$$\mathbf{T}^T_{CB}\mathbf{K}\mathbf{T}_{CB} = \begin{bmatrix} \mathbf{K}_{RR} - \mathbf{K}_{RC}\mathbf{K}^{-1}_{CC}\mathbf{K}_{CR} & \mathbf{0} \\ \mathbf{0} & \mathbf{\Omega}^2_{CNM} \end{bmatrix} \tag{43}$$

and

$$\mathbf{T}^T_{CB}\mathbf{M}\mathbf{T}_{CB} = \begin{bmatrix} \widetilde{\mathbf{M}}_{RR} & \widetilde{\mathbf{M}}_{RC} \\ \widetilde{\mathbf{M}}_{CR} & \mathbf{I} \end{bmatrix}, \tag{44}$$

where

$$\widetilde{\mathbf{M}}_{RR} = \mathbf{M}_{RR} - \mathbf{M}_{RC}\mathbf{K}^{-1}_{CC}\mathbf{K}_{CR} - \mathbf{K}_{RC}\mathbf{K}^{-1}_{CC}\mathbf{M}_{CR} + \mathbf{K}_{RC}\mathbf{K}^{-1}_{CC}\mathbf{M}_{CC}\mathbf{K}^{-1}_{CC}\mathbf{K}_{CR} \tag{45}$$

and

$$\widetilde{\mathbf{M}}_{CR} = \widetilde{\mathbf{M}}^T_{RC} = \mathbf{\Phi}^T_{CNM}\left(\mathbf{M}_{CR} - \mathbf{M}_{CC}\mathbf{K}^{-1}_{CC}\mathbf{K}_{CR}\right). \tag{46}$$

4.2. Craig-Bampton model with imposed acceleration

When the retained DoFs consist only of boundary DoFs, Equation (43) shows that there is no stiffness coupling term between the boundary and internal DoFs. Imposing accelerations to the retained DoFs of a Craig-Bampton reduced-order model is thus a straightforward procedure.

When there are more DoFs than the boundary ones in the retained DoFs however, a non-zero static coupling term exists because the matrix $\mathbf{K}_{RR} - \mathbf{K}_{RC}\mathbf{K}^{-1}_{CC}\mathbf{K}_{CR}$ is full in general. Any procedure outlined in Section 3.1 can then be used.

4.3. Craig-Bampton model with imposed displacement

In contrast with the case of imposed acceleration, a Craig-Bampton ROM does not lend itself to the case of imposed displacement, and the methods presented in Section 3.2 are then to be used, even when the retained DoFs only consist of boundary ones. Indeed, the mass matrix is far from being close to block-diagonal; neglecting the off-diagonal terms can lead to a substantial error, as shall be illustrated in Section 7.

It should also be noted that the reduced matrices resulting from the RAM applied to Craig-Bampton ROMs with identical retained and boundary DoFs were recently presented in the literature, although in a completely different context. In [36], a so-called massless Craig-Bampton method was proposed using the reduction matrix

$$\mathbf{T}_{MCB} = \begin{bmatrix} \mathbf{I} & \mathbf{0} \\ -\mathbf{K}_{CC}^{-1}\mathbf{K}_{CR} - \boldsymbol{\Phi}_{CNM}\boldsymbol{\Phi}_{CNM}^{T}\left(\mathbf{M}_{CR} - \mathbf{M}_{CC}\mathbf{K}_{CC}^{-1}\mathbf{K}_{CR}\right) & \boldsymbol{\Phi}_{CNM} \end{bmatrix} \tag{47}$$

with the aim to simplify the computation of vibro-impact processes. Using Equations (30) (choosing $\mathbf{T}_{I,d} = \mathbf{I}$), (42), (44) and (46), this reduction matrix can equivalently be expressed by

$$\begin{aligned} \mathbf{T}_{MCB} &= \begin{bmatrix} \mathbf{I} & \mathbf{0} \\ -\mathbf{K}_{CC}^{-1}\mathbf{K}_{CR} & \boldsymbol{\Phi}_{CNM} \end{bmatrix} \begin{bmatrix} \mathbf{I} & \mathbf{0} \\ -\boldsymbol{\Phi}_{CNM}^{T}\left(\mathbf{M}_{CR} - \mathbf{M}_{CC}\mathbf{K}_{CC}^{-1}\mathbf{K}_{CR}\right) & \mathbf{I} \end{bmatrix} \\ &= \mathbf{T}_{CB} \begin{bmatrix} \mathbf{I} & \mathbf{0} \\ -\widetilde{\mathbf{M}}_{CR} & \mathbf{I} \end{bmatrix} = \mathbf{T}_{CB}\mathbf{T}_{RAM} \end{aligned} \tag{48}$$

This decomposition indicates that the reduction proposed in [36] is identical to the RAM applied to the Craig-Bampton reduced model when retained DoFs are only boundary ones. We also note that the transformation proposed in [36] under the formulation proposed herein can be performed from a classical Craig-Bampton reduced model and thus does not require the knowledge of the full FE matrices, which are seldom available in commercial FE software.

4.4. Other types of reduced-order model

Reduced-order models based on free-interface modes are less common than the Craig-Bampton ones, and are thus only briefly discussed here for completeness.

In MacNeal's method [15], the mass matrix exhibits the simple structure [7, 36]

$$\mathbf{M}_{MN} = \begin{bmatrix} \mathbf{0} & \mathbf{0} \\ \mathbf{0} & \mathbf{I} \end{bmatrix}, \tag{49}$$

(where subscript MN is used for MacNeal) which allows for a straightforward imposition of prescribed displacements. This simplicity comes at the expense of an inconsistent mass matrix. Its consistent counterpart, Rubin's method [16], features mass and stiffness matrices which are both full. In this case, any of the methods presented in Section 3 can nonetheless be used to prescribe boundary motion. The same remark also applies to ROMs which express the reduced dynamics in the same fashion as Equation (4).

5. State-space models

As discussed in the introduction, state-space models are largely used in various system identification approaches and in the active control community. Furthermore, damping can be handled more naturally with such a formulation. The models developed herein are thus adapted to a state-space formulation in this section.

5.1. State-space models of structures with external forcing

It is now considered that the external forcing can be described by

$$\mathbf{f} = \mathbf{B}_f \mathbf{u}_f, \tag{50}$$

where $\mathbf{B}_f$ is a matrix whose columns indicate the spatial distribution of the different independent forcings under consideration, and $\mathbf{u}_f$ is a vector containing their time-dependent amplitudes. From Equation (4) (or any similar model after reduction), an equivalent set of first-order ODEs can be obtained as

$$\begin{bmatrix} \dot{\mathbf{q}} \\ \ddot{\mathbf{q}} \end{bmatrix} = \begin{bmatrix} \mathbf{0} & \mathbf{I} \\ -\mathbf{M}^{-1}\mathbf{K} & \mathbf{0} \end{bmatrix} \begin{bmatrix} \mathbf{q} \\ \dot{\mathbf{q}} \end{bmatrix} + \begin{bmatrix} \mathbf{0} \\ \mathbf{M}^{-1}\mathbf{B}_f \end{bmatrix} \mathbf{u}_f. \tag{51}$$

This is then equivalent to a state evolution equation with the state and input vectors $\begin{bmatrix} \mathbf{q}^T & \dot{\mathbf{q}}^T \end{bmatrix}^T$ and $\mathbf{u}_f$, respectively. Other transformations that yield symmetric state-space matrices can be used (see, e.g., [7, 24]).

A more computationally efficient method consists in using the modes of the structure. Assuming that the mode shapes are mass-normalized, the modes are defined by the equations

$$\mathbf{q} = \mathbf{\Phi}\boldsymbol{\eta}, \qquad \mathbf{M}\mathbf{\Phi}\mathbf{\Omega}^2 = \mathbf{K}\mathbf{\Phi}, \qquad \mathbf{\Phi}^T\mathbf{M}\mathbf{\Phi} = \mathbf{I}, \tag{52}$$

where $\mathbf{\Phi}$ is a mode shape matrix, $\boldsymbol{\eta}$ are modal coordinates and $\mathbf{\Omega}$ is a diagonal matrix containing the circular resonance frequencies. With Equation (52), the premultiplication of Equation (4) by $\mathbf{\Phi}^T$ reads

$$\ddot{\boldsymbol{\eta}} + \mathbf{\Omega}^2\boldsymbol{\eta} = \mathbf{\Phi}^T\mathbf{B}_f\mathbf{u}_f. \tag{53}$$

Damping can readily be added to the model at this stage using a diagonal matrix of modal damping ratios $\mathbf{Z}$. The modal equations of motion are then given by

$$\ddot{\boldsymbol{\eta}} + 2\mathbf{Z}\mathbf{\Omega}\dot{\boldsymbol{\eta}} + \mathbf{\Omega}^2\boldsymbol{\eta} = \mathbf{\Phi}^T\mathbf{B}_f\mathbf{u}_f. \tag{54}$$

This yields the state evolution equation

$$\begin{bmatrix} \dot{\boldsymbol{\eta}} \\ \ddot{\boldsymbol{\eta}} \end{bmatrix} = \begin{bmatrix} \mathbf{0} & \mathbf{I} \\ -\mathbf{\Omega}^2 & -2\mathbf{Z}\mathbf{\Omega} \end{bmatrix} \begin{bmatrix} \boldsymbol{\eta} \\ \dot{\boldsymbol{\eta}} \end{bmatrix} + \begin{bmatrix} \mathbf{0} \\ \mathbf{\Phi}^T\mathbf{B}_f \end{bmatrix} \mathbf{u}_f, \tag{55}$$

in which the states are coupled only by pairs, since the modes are decoupled in Equation (54). The output equation depends on the outputs desired by the user. For instance, if one specifies the output as a combination of the generalized DoFs by

$$\mathbf{y} = \mathbf{C}\mathbf{q}, \tag{56}$$

then, with Equation (52), the state-space output equation is given by

$$\mathbf{y} = \begin{bmatrix} \mathbf{C}\mathbf{\Phi} & \mathbf{0} \end{bmatrix} \begin{bmatrix} \boldsymbol{\eta} \\ \dot{\boldsymbol{\eta}} \end{bmatrix}, \tag{57}$$

thereby fully specifying the state-space model of the structure (Equations (55) and (57)).

5.2. Model reduction during the state-space construction

Model order reduction can also be performed during the state-space model construction. Such a reduction can be based on the modes of the structure defined in Equation (52). A partition of the modes can be performed as

$$\boldsymbol{\Phi}\boldsymbol{\eta} = \begin{bmatrix}\boldsymbol{\Phi}_R & \boldsymbol{\Phi}_D\end{bmatrix}\begin{bmatrix}\boldsymbol{\eta}_R \\ \boldsymbol{\eta}_D\end{bmatrix}, \tag{58}$$

where subscripts R and D stand for retained and discarded, respectively. Since the modal equations are uncoupled, their state evolution equation is simply obtained by truncating Equation (55) as

$$\begin{bmatrix}\dot{\boldsymbol{\eta}}_R \\ \ddot{\boldsymbol{\eta}}_R\end{bmatrix} = \begin{bmatrix}\mathbf{0} & \mathbf{I} \\ -\boldsymbol{\Omega}_R^2 & -2\mathbf{Z}_R\boldsymbol{\Omega}_R\end{bmatrix}\begin{bmatrix}\boldsymbol{\eta}_R \\ \dot{\boldsymbol{\eta}}_R\end{bmatrix} + \begin{bmatrix}\mathbf{0} \\ \boldsymbol{\Phi}_R^T\mathbf{B}_f\end{bmatrix}\mathbf{u}_f. \tag{59}$$

There exists different approaches to select these retained modal coordinates. For instance, one may retain modes whose frequencies are up to 1.5 times the highest frequency of interest [16]. This factor be made closer to one if a static correction is added as well, a procedure which will be detailed hereafter. Another basis than the modes of the structure can also be selected for reduction, but this aspect is not treated herein (except for residual attachment modes, see below).

In order to add a static correction, the discarded modal coordinates $\boldsymbol{\eta}_D$ are assumed to respond quasi-statically. Equation (54) then becomes for these modal coordinates

$$\boldsymbol{\Omega}_D^2\boldsymbol{\eta}_D = \boldsymbol{\Phi}_D^T\mathbf{B}_f\mathbf{u}_f. \tag{60}$$

From Equation (52), the generalized DoFs can be reconstructed as

$$\mathbf{q} = \boldsymbol{\Phi}_R\boldsymbol{\eta}_R + \boldsymbol{\Phi}_D\boldsymbol{\eta}_D = \boldsymbol{\Phi}_R\boldsymbol{\eta}_R + \boldsymbol{\Phi}_D\boldsymbol{\Omega}_D^{-2}\boldsymbol{\Phi}_D^T\mathbf{B}_f\mathbf{u}_f. \tag{61}$$

In practice, the discarded modes need not be computed. Indeed, from Equation (52), it can be derived that the inverse of the stiffness matrix admits the modal expansion [7]

$$\mathbf{K}^{-1} = \boldsymbol{\Phi}\boldsymbol{\Omega}^{-2}\boldsymbol{\Phi}^T = \boldsymbol{\Phi}_R\boldsymbol{\Omega}_R^{-2}\boldsymbol{\Phi}_R^T + \boldsymbol{\Phi}_D\boldsymbol{\Omega}_D^{-2}\boldsymbol{\Phi}_D^T, \tag{62}$$

and therefore Equation (61) becomes

$$\mathbf{q} = \boldsymbol{\Phi}_R\boldsymbol{\eta}_R + \left(\mathbf{K}^{-1} - \boldsymbol{\Phi}_R\boldsymbol{\Omega}_R^{-2}\boldsymbol{\Phi}_R^T\right)\mathbf{B}_f\mathbf{u}_f, \tag{63}$$

showing that the externally-excited structure can be described through its retained and residual attachment modes. The latter are defined by the columns of the matrix premultiplying $\mathbf{u}_f$ [37]. They correspond to the static structural response, from which the contribution of the retained modes has been removed, when an external force is applied to the structure with a spatial distribution given by a column of $\mathbf{B}_f$. For structures with rigid body modes, $\mathbf{K}$ is singular, and one must resort to the computation of inertia-relief attachment modes [37].

With these residual attachment modes, two approaches can be followed to add a static correction to the model: one can either include these modes into the reduction basis, or take their effect into account with a feedthrough term in the state-space model, as detailed below.

5.2.1. Model with residual attachment modes

The reduction basis with $\boldsymbol{\Phi}_R$ can be complemented by the residual attachment modes, defining a reduction matrix

$$\mathbf{T}_{RA} = \begin{bmatrix} \boldsymbol{\Phi}_R & \left(\mathbf{K}^{-1} - \boldsymbol{\Phi}_R \boldsymbol{\Omega}_R^{-2} \boldsymbol{\Phi}_R^T\right) \mathbf{B}_f \end{bmatrix}, \tag{64}$$

and adding other DoFs to the models. In practice, this reduction matrix is orthogonalized to improve numerical conditioning. The resulting ROM is statically exact and the static correction makes it very accurate in the frequency range of the retained modes. As a final step, one can compute the normal modes of this reduced model to obtain a state-space model with decoupled states, in the form of Equation (55).

5.2.2. Model with feedthrough term

An alternative to using residual attachment modes is to consider their effect through a feedthrough term in the state-space model. In this approach, only the retained modal coordinates $\boldsymbol{\eta}_R$ are used as state variables. Using Equation (63) the state-space output equation (Equation (56)) becomes

$$\mathbf{y} = \begin{bmatrix} \mathbf{C}\boldsymbol{\Phi}_R & \mathbf{0} \end{bmatrix} \begin{bmatrix} \boldsymbol{\eta}_R \\ \dot{\boldsymbol{\eta}}_R \end{bmatrix} + \mathbf{C} \left(\mathbf{K}^{-1} - \boldsymbol{\Phi}_R \boldsymbol{\Omega}_R^{-2} \boldsymbol{\Phi}_R^T\right) \mathbf{B}_f \mathbf{u}_f, \tag{65}$$

featuring a feedthrough matrix

$$\mathbf{D} = \mathbf{C} \left(\mathbf{K}^{-1} - \boldsymbol{\Phi}_R \boldsymbol{\Omega}_R^{-2} \boldsymbol{\Phi}_R^T\right) \mathbf{B}_f \tag{66}$$

that is due to the residual flexibility of the discarded modes. The advantage of this approach is that it does not introduce more states than those associated with the retained modal coordinates. However, the presence of a feedthrough matrix can lead to non-physical results, such as an instantaneous response to an input in wave propagation problems.

5.3. State-space models with the direct approach

The remainder of this section now considers imposed boundary accelerations or displacements. For simplicity, other external forcings are disregarded (in particular, it is considered that $\mathbf{f}_I = \mathbf{0}$). The models can nonetheless easily be adapted if these forcings are to be accounted for.

A state-space model can be built from Equation (11) (or any reduced version of it) by considering the inertia and stiffness forces imparted by the boundary DoFs motion as independent inputs to the state-space model. Using the modes of the structure with fixed boundary DoFs defined by

$$\mathbf{q}_I = \boldsymbol{\Phi}_I \boldsymbol{\eta}_I, \qquad \mathbf{M}_{II} \boldsymbol{\Phi}_I \boldsymbol{\Omega}_I^2 = \mathbf{K}_{II} \boldsymbol{\Phi}_I, \qquad \boldsymbol{\Phi}_I^T \mathbf{M}_{II} \boldsymbol{\Phi}_I = \mathbf{I}, \tag{67}$$

where $\boldsymbol{\Phi}_I$ is a mode shape matrix, $\boldsymbol{\eta}_I$ are modal coordinates and $\boldsymbol{\Omega}_I$ is a diagonal matrix containing the circular resonance frequencies, and introducing a diagonal matrix of modal damping ratios $\mathbf{Z}_I$, the state evolution equation reads

$$\begin{bmatrix} \dot{\boldsymbol{\eta}}_I \\ \ddot{\boldsymbol{\eta}}_I \end{bmatrix} = \begin{bmatrix} \mathbf{0} & \mathbf{I} \\ -\boldsymbol{\Omega}_I^2 & -2\mathbf{Z}_I \boldsymbol{\Omega}_I \end{bmatrix} \begin{bmatrix} \boldsymbol{\eta}_I \\ \dot{\boldsymbol{\eta}}_I \end{bmatrix} + \begin{bmatrix} \mathbf{0} & \mathbf{0} \\ -\boldsymbol{\Phi}_I^T \mathbf{K}_{IB} & -\boldsymbol{\Phi}_I^T \mathbf{M}_{IB} \end{bmatrix} \begin{bmatrix} \mathbf{q}_P \\ \ddot{\mathbf{q}}_P \end{bmatrix}. \tag{68}$$

We note that in this case the fixed-interface modes are considered (in contrast to the free-interface modes in Equation (52)) because the structural matrices in Equation (11) are associated with the structure with fixed interfaces. More generally, modes can be selected based on the mass and stiffness matrices associated with the equations governing the dynamics of the unknown DoFs.

Static corrections can be added to the model as well. Since the right-hand side of Equation (11) (still considering $\mathbf{f}_I = \mathbf{0}$) can be written as

$$-\mathbf{M}_{IB}\ddot{\mathbf{q}}_P - \mathbf{K}_{IB}\mathbf{q}_P = \begin{bmatrix}-\mathbf{K}_{IB} & -\mathbf{M}_{IB}\end{bmatrix}\begin{bmatrix}\mathbf{q}_P \\ \ddot{\mathbf{q}}_P\end{bmatrix}, \tag{69}$$

the first and second matrices in the right-hand side of this equation can be treated as $\mathbf{B}_f$ and $\mathbf{u}_f$, respectively, in the procedures outlined in Sections 5.2.1 and 5.2.2.

Again, alternatives where only the prescribed displacements or accelerations are required are analyzed in the sequel.

5.4. State-space models of structures with imposed acceleration

The methods reviewed in Section 3.1 all result in a model of the form

$$\mathbf{M}_a\ddot{\mathbf{x}}_a + \mathbf{K}_a\mathbf{x}_a = \mathbf{B}_a\ddot{\mathbf{q}}_P, \tag{70}$$

where $\mathbf{M}_a$, $\mathbf{K}_a$, $\mathbf{B}_a$ and $\mathbf{x}_a$ depend on the chosen method. One observes that the term $\mathbf{B}_a\ddot{\mathbf{q}}_P$ plays the same role as an external forcing, and Equation (70) has the same structure as Equation (4). The procedure outlined in Section 5.1 can thus be followed (substituting the quantities in Equation (4) by their counterparts in Equation (70)) to yield the state-space model

$$\begin{bmatrix}\dot{\boldsymbol{\eta}}_a \\ \ddot{\boldsymbol{\eta}}_a\end{bmatrix} = \begin{bmatrix}\mathbf{0} & \mathbf{I} \\ -\boldsymbol{\Omega}_a^2 & -2\mathbf{Z}_a\boldsymbol{\Omega}_a\end{bmatrix}\begin{bmatrix}\boldsymbol{\eta}_a \\ \dot{\boldsymbol{\eta}}_a\end{bmatrix} + \begin{bmatrix}\mathbf{0} \\ \boldsymbol{\Phi}_a^T\mathbf{B}_a\end{bmatrix}\ddot{\mathbf{q}}_P, \tag{71}$$

where $\boldsymbol{\Omega}_a$ and $\boldsymbol{\Phi}_a$ are computed from Equation (52) by replacing $\mathbf{M}$ and $\mathbf{K}$ by $\mathbf{M}_a$ and $\mathbf{K}_a$, respectively, $\boldsymbol{\eta}_a$ is the associated vector of modal coordinates, and $\mathbf{Z}_a$ is a diagonal matrix of modal damping ratios. The interpretation of these modes depend on the selected method. If a static correction is to be added to the model, the procedures outlined in Sections 5.2.1 and 5.2.2 can be followed by replacing $\mathbf{B}_f$ by $\mathbf{B}_a$.

Regarding the direct method outlined in Section 3.1.1, the procedure requires a slight adaptation because the structural matrices are nonsymmetric. The modes associated to Equation (12) are found to be

$$\begin{bmatrix}\mathbf{q}_B \\ \mathbf{q}_I\end{bmatrix} = \begin{bmatrix}\mathbf{I} & \mathbf{0} \\ -\mathbf{K}_{II}^{-1}\mathbf{K}_{IB} & \boldsymbol{\Phi}_I\end{bmatrix}\begin{bmatrix}\mathbf{q}_B \\ \boldsymbol{\eta}_I\end{bmatrix}. \tag{72}$$

Inserting this transformation into Equation (12) and premultiplying it by

$$\begin{bmatrix}\mathbf{I} & \mathbf{0} \\ \mathbf{0} & \boldsymbol{\Phi}_I\end{bmatrix} \tag{73}$$

yields the equivalent state-space evolution equation (with introduction of modal damping)

$$\begin{bmatrix}\dot{\mathbf{q}}_B \\ \dot{\boldsymbol{\eta}}_I \\ \ddot{\mathbf{q}}_B \\ \ddot{\boldsymbol{\eta}}_I\end{bmatrix} = \begin{bmatrix}\mathbf{0} & \mathbf{0} & \mathbf{I} & \mathbf{0} \\ \mathbf{0} & \mathbf{0} & \mathbf{0} & \mathbf{I} \\ \mathbf{0} & \mathbf{0} & \mathbf{0} & \mathbf{0} \\ -\boldsymbol{\Phi}_I^T\mathbf{K}_{IB} & -\boldsymbol{\Omega}_I^2 & \mathbf{0} & -2\mathbf{Z}_I\boldsymbol{\Omega}_I\end{bmatrix}\begin{bmatrix}\mathbf{q}_B \\ \boldsymbol{\eta}_I \\ \dot{\mathbf{q}}_B \\ \dot{\boldsymbol{\eta}}_I\end{bmatrix} + \begin{bmatrix}\mathbf{0} \\ \mathbf{0} \\ \mathbf{I} \\ -\boldsymbol{\Phi}_I^T\mathbf{M}_{IB}\end{bmatrix}\ddot{\mathbf{q}}_P, \tag{74}$$

showing that the system input $\ddot{\mathbf{q}}_P$ is integrated twice to yield the state $\mathbf{q}_B$, which is then used in the modal dynamic equilibrium equation. The matrices in Equations (72) and (73) can be seen

as defining the right and left eigenvectors, respectively, of a nonsymmetric generalized eigenvalue problem associated with the nonsymmetric matrices in Equation (12).

The difference between Equations (71) and (74) lies in the states of the system, which depend on the chosen method for imposed acceleration. When one works with the RAM (or with a rigid support motion), Equation (71) results in a system with less states because only the relative motion information is retained. However, storing all states with Equation (74) can be advantageous in some cases, e.g., when one wants to compute absolute displacements.

Finally, it should be noted that the proposed method seamlessly introduces modal damping on selected modes. In particular, damping introduction into the LMM model causes no issues. By contrast, introducing it via Rayleigh damping in a structural model may cause potential issues if not handled carefully [12].

5.5. State-space models of structures with imposed displacement

The methods reviewed in Section 3.2 all result in a model of the form

$$\mathbf{M}_d\ddot{\mathbf{x}}_d + \mathbf{K}_d\mathbf{x}_d = \mathbf{B}_d\mathbf{q}_P, \tag{75}$$

where again $\mathbf{M}_d$, $\mathbf{K}_d$, $\mathbf{B}_d$ and $\mathbf{x}_d$ are method-dependent. Following the approach outlined in Section 5.1 (substituting the quantities in Equation (4) by their counterparts in Equation (75)), a state evolution equation is obtained as

$$\begin{bmatrix}\dot{\boldsymbol{\eta}}_d \\ \ddot{\boldsymbol{\eta}}_d\end{bmatrix} = \begin{bmatrix}\mathbf{0} & \mathbf{I} \\ -\boldsymbol{\Omega}_d^2 & -2\mathbf{Z}_d\boldsymbol{\Omega}_d\end{bmatrix}\begin{bmatrix}\boldsymbol{\eta}_d \\ \dot{\boldsymbol{\eta}}_d\end{bmatrix} + \begin{bmatrix}\mathbf{0} \\ \boldsymbol{\Phi}_d^T\mathbf{B}_d\end{bmatrix}\mathbf{q}_P, \tag{76}$$

where $\boldsymbol{\Omega}_d$ and $\boldsymbol{\Phi}_d$ are computed from Equation (52) by replacing $\mathbf{M}$ and $\mathbf{K}$ by $\mathbf{M}_d$ and $\mathbf{K}_d$, respectively, $\boldsymbol{\eta}_d$ is the associated vector of modal coordinates, and $\mathbf{Z}_d$ is a diagonal matrix of modal damping ratios. Once again, the interpretation of these modes is method-dependent. We also note that adding a static correction to the model is simply performed by replacing $\mathbf{B}_f$ by $\mathbf{B}_d$ in the procedures outlined in Sections 5.2.1 and 5.2.2.

The formulation with a direct method when the mass matrix is (considered) diagonal can be obtained from Equation (68) by simply removing the input $\ddot{\mathbf{q}}_P$.

When using the direct method with a non-block-diagonal mass matrix or the Lagrange multipliers method, the mass matrices are singular (Equations (27) and (38)). This prevents the construction of a state-space model using the formulation in Equation (51). As for the associated modal model in Equation (76), the singularity of the mass matrix translates into infinite frequencies in the matrix $\boldsymbol{\Omega}_d$. These approaches are therefore not suited for use with state-space models.

5.6. Discussion

To conclude this section, extensions of this work that could benefit from the developments of this section are discussed.

In this work, modal damping was introduced in the model for simplicity. General viscous damping models could be considered without great difficulty. State decoupling would be achievable using complex modes [7, 24], thereby providing an efficient approach to compute the structural frequency response.

With the state-space models developed herein, structural assembly can easily be performed as the state-space models of the assembled substructures just need to be connected in cascade. Thus, the method proposed in [32] can be applied directly, without need for any state transformation.

There exist several competitive system identification techniques working with state-space models (e.g. [26]), and an application to systems excited by seismic motions was discussed in [38]. With the identified models, modes can easily be computed, but their relation to the structural properties may not be obvious. The models developed herein give an interpretation of these modes. This could be used in a finite element model updating context. For instance, the system equivalent reduction expansion process [39] could use the assumed mode shapes. This could offer an interesting alternative to the method proposed in [38].

6. Summary

The procedure to build a state-space model of a structure with imposed acceleration or displacement is summarized as follows:

1. Build a FE model of a structure.
2. Optionally, use a classical reduction approach, such as the Craig-Bampton method (see Section 4).
3. Transform or augment the model following methods for imposed acceleration (see Section 3.1) or displacements (see Section 3.2).
4. Build a state-space model of the structure (see Section 5.1), with an optional reduction step and an optional static correction (see Section 5.2).

7. Examples

The proposed methods are illustrated with three examples of increasing complexity. The first example is a bar in extension used to gain insight about the newly proposed RAM. A cantilever beam is then studied to compare the different methods. Finally, the case of a multi-story building model with a large number of DoFs is analyzed. In the two first examples, the accuracy of the various methods is evaluated through their relative error given by

$$e(\omega) = \left| \frac{q_{ref}(\omega) - q_m(\omega)}{q_{ref}(\omega)} \right|, \tag{77}$$

where $q_{ref}(\omega)$ is the reference solution obtained from the direct method applied to the full model, $q_m(\omega)$ is the solution given by the considered method, and $|\cdot|$ denotes the absolute value. Unless otherwise stated, the state-space ROMs include a static correction via a feedthrough term.

7.1. Bar in extension

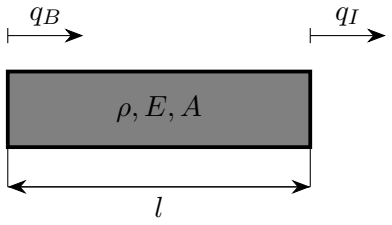

Figure 2: Base-excited bar.

One of the simplest examples to illustrate the proposed approaches is a finite element model of a bar in extension with one element, as illustrated in Figure 2. Using a Galerkin approach with linear shape functions to discretize the displacement field, the mass and stiffness matrices of this bar element are given by

$$\mathbf{M} = \frac{\rho A l}{6}\begin{bmatrix} 2 & 1 \\ 1 & 2 \end{bmatrix}, \qquad \mathbf{K} = \frac{EA}{l}\begin{bmatrix} 1 & -1 \\ -1 & 1 \end{bmatrix}, \tag{78}$$

where l and A are the length and cross-section area of the bar, respectively, and ρ and E are the material's density and Young's modulus [7]. This free-free bar model has two resonance frequencies: 0, which corresponds to a rigid body mode, and $\sqrt{3E/(\rho l^2)}$, which is used to normalize all frequencies in this example.

From Equations (15) and (78), the RMM transformation matrix is given by

$$\mathbf{T}_{RMM} = \begin{bmatrix} 1 & 0 \\ 1 & 1 \end{bmatrix}, \tag{79}$$

changing the degrees of freedom to the base motion q_B and a relative motion $q_I - q_B$. This yields the transformed mass and stiffness matrices as

$$\mathbf{M}_{RMM} = \frac{\rho A l}{6}\begin{bmatrix} 6 & 3 \\ 3 & 2 \end{bmatrix}, \qquad \mathbf{K}_{RMM} = \frac{EA}{l}\begin{bmatrix} 0 & 0 \\ 0 & 1 \end{bmatrix}, \tag{80}$$

respectively. As for the RAM transformation matrix, Equations (30) and (78) result in

$$\mathbf{T}_{RAM} = \begin{bmatrix} 1 & 0 \\ -1/2 & 1 \end{bmatrix}, \tag{81}$$

which allows for the computation of the transformed mass and stiffness matrices as

$$\mathbf{M}_{RAM} = \frac{\rho A l}{6}\begin{bmatrix} 3/2 & 0 \\ 0 & 2 \end{bmatrix}, \qquad \mathbf{K}_{RAM} = \frac{EA}{l}\begin{bmatrix} 9/4 & -3/2 \\ -3/2 & 1 \end{bmatrix}. \tag{82}$$

A mass lumping procedure can also be adopted. Half the total mass of the bar is attributed to each node, resulting in the diagonal mass matrix

$$\mathbf{M}_l = \frac{\rho A l}{2}\begin{bmatrix} 1 & 0 \\ 0 & 1 \end{bmatrix}. \tag{83}$$

This mass lumping procedure makes the bar model qualitatively equivalent to a spring-mass model.

A longitudinal unit-amplitude harmonic displacement is prescribed on q_B, hence

$$q_P(t) = \cos(\omega t), \qquad \ddot{q}_P(t) = -\omega^2 \cos(\omega t). \tag{84}$$

Figure 3a depicts the transmissibilities obtained with various methods. Among them, the RMM and RAM agree perfectly with the direct method (Equation (11)). On the contrary, the mass lumping approximation features a large error at and above the bar resonance frequency, and underestimates the transmissibility at high frequencies. Assuming a static coupling, i.e., neglecting the inertial coupling term in Equation (11) appears to be a better approximation around resonance. However, discrepancies are still visible, and the approximation performs poorly at high frequencies. The

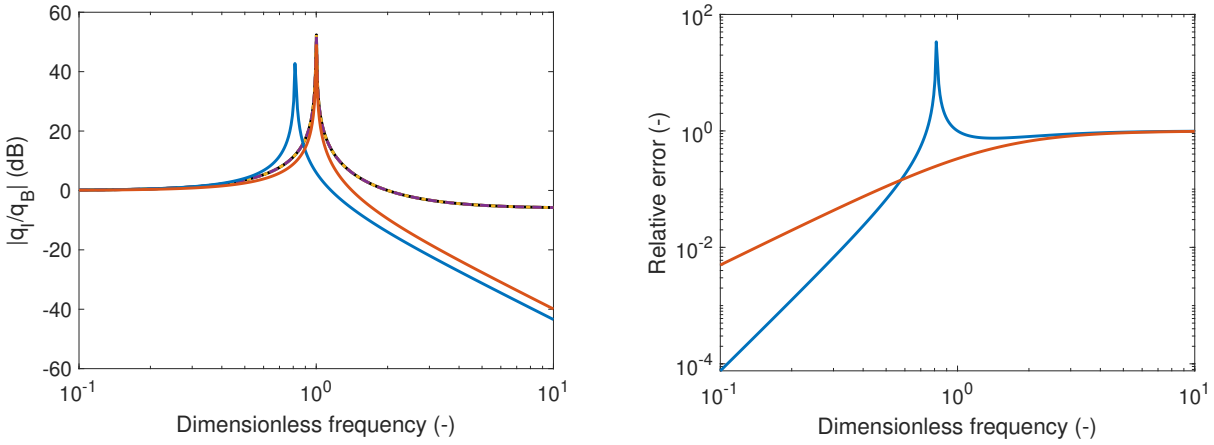

(a) (b)

Figure 3: Base-excited bar with one element: transmissibility with the direct method (—), RMM (-·-), RAM (- - -), mass lumping (—) and static coupling approximation (—) (a), and relative error of the mass lumping (—) and static coupling (—) approximations (b).

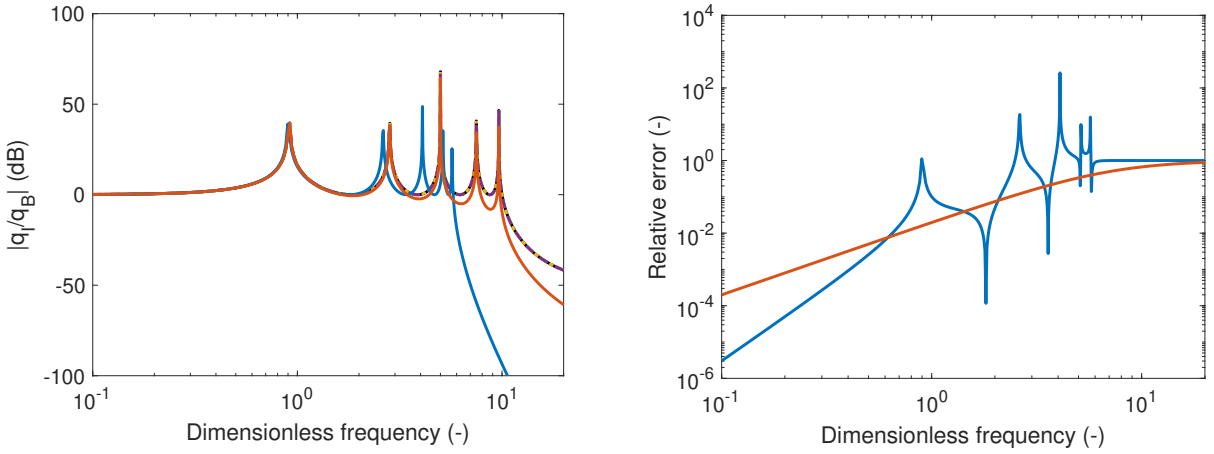

(a) (b)

Figure 4: Base-excited bar with five elements: transmissibility with the direct method (—), RMM (-·-), RAM (- - -), mass lumping (—) and static coupling approximation (—) methods (a), and relative error of the mass lumping (—) and static coupling (—) approximations (b).

relative errors of the two approximation methods are reported in Figure 3b. The mass lumping approximation performs better than the static coupling approximation at low frequencies.

Extending the results to a discretization with five elements, Figure 4a displays the transmissibilities obtained with the same methods. Once again, there is a perfect agreement with the direct, RMM and RAM methods. This time, the mass lumping and static coupling approximations provide a satisfactory evaluation of the transmissibility around the first resonance. Because the mass lumping method underestimates the resonance frequencies of the model, it performs poorly around these misevaluated resonance frequencies, as can be seen in Figure 4b. Yet, it outperforms the static coupling approach at low frequencies.

In an attempt to understand the coordinate transformations in the RMM and RAM methods,

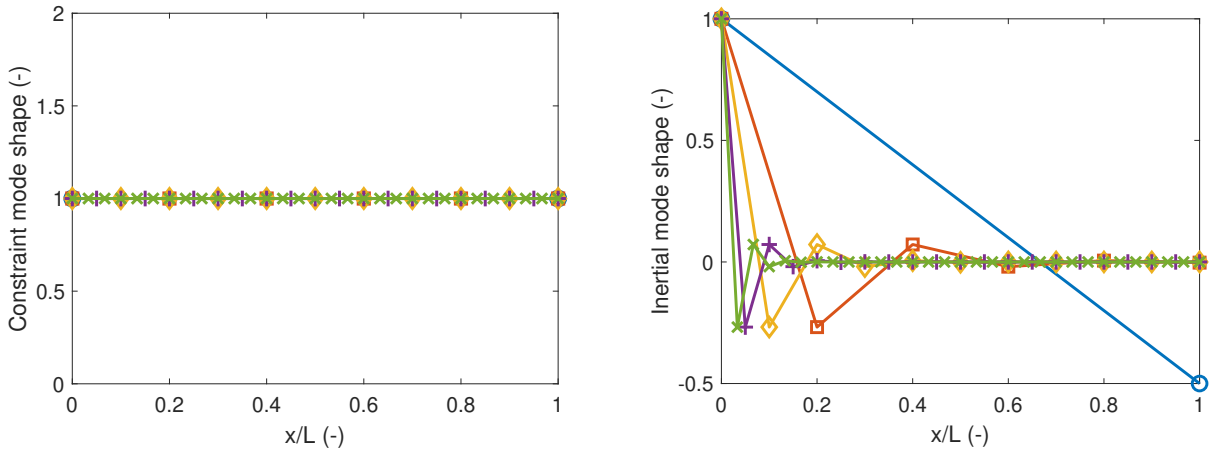

(a) (b)

Figure 5: First column of the RMM (a) and RAM (b) transformation matrices for a bar with 1 (○), 5 (□), 10 (◇), 20 (+) and 30 (×) elements.

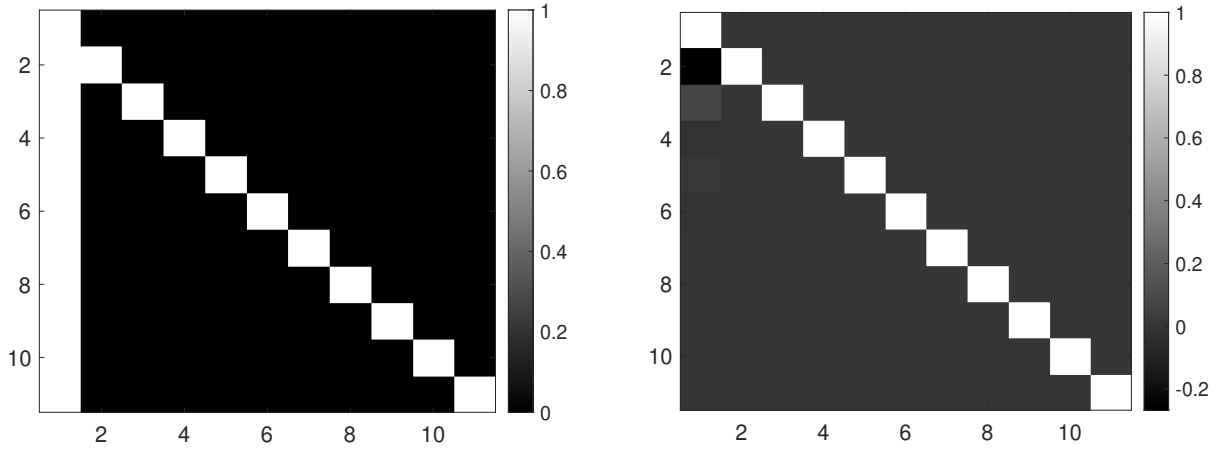

(a) (b)

Figure 6: RMM (a) and RAM (b) transformation matrices for a bar with ten elements.

Figure 5 plots the first column of the transformation matrices for various number of elements. With the RMM method, a rigid-body mode is recognized in Figure 5a. According to the discussion in Section 3.1.2, this is to be expected, because in this case a rigid motion is imposed to the base. The constraint mode is thus a rigid-body mode, and the remaining coordinates describe a motion relative to the base motion, which is confirmed by looking at the RMM transformation matrix (Equation (15) with $\mathbf{T}_{I,d} = \mathbf{I}$) for a case with ten elements in Figure 6a.

By contrast, the first column of the RAM transformation matrix does not converge uniformly to a specific deformation as shown in Figure 5b. This is particularly observable for the DoFs closest to the boundary. However, a convergence toward a zero motion is observable for the DoFs close to the free end. Hence, the transformed DoFs tend to represent absolute coordinates. This is also confirmed by looking at the transformation matrix (Equation (30) with $\mathbf{T}_{I,d} = \mathbf{I}$) for the case with ten elements in Figure 6b, for which the lower block tends to resemble the concatenation of a zero

matrix and an identity matrix. In conclusion, it appears that the coordinate transformation tends to a formulation where absolute displacements are used, without being ever fully equivalent to it if the mass matrix is not diagonal, because it needs to perform a mass decoupling action between the boundary and internal DoFs. The extent to which it differs from a formulation with absolute displacement depends on the discretization.

7.2. Cantilever beam

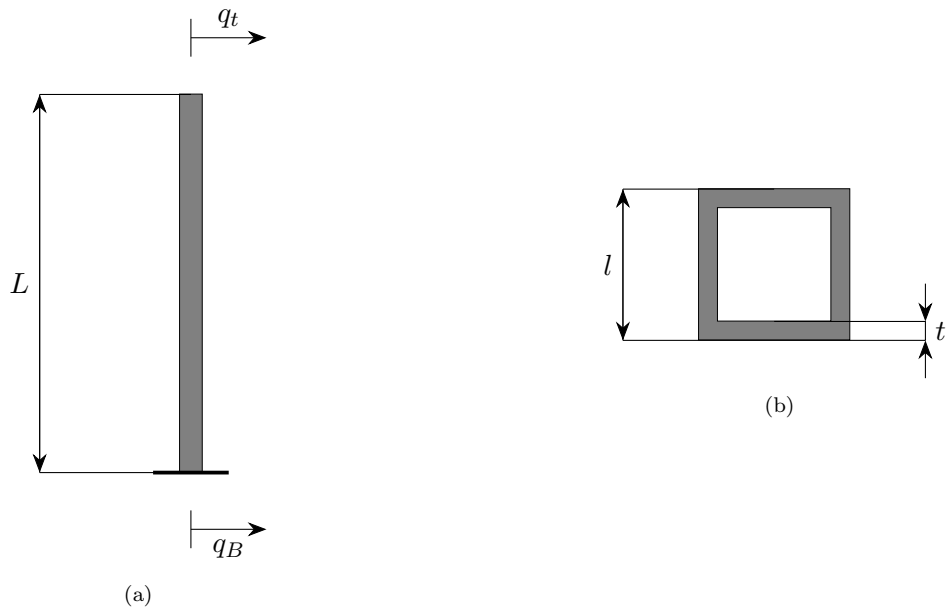

Figure 7: Base-excited cantilever beam: front view (a) and cross-sectional view (b).

A concrete cantilever beam with a square hollow section depicted in Figure 7 is now studied. The material behavior is assumed to be linear, isotropic and elastic. Table 1 reports the geometric and material characteristics of the beam. Its model was built with 20 Euler-Bernoulli elements using the Structural Dynamics Toolbox (SDT) in MATLAB [40]. The response of the beam is assessed through its transversal tip displacement q_t.

L	l	t	E	ν	ρ
140m	20m	30cm	30GPa	0.2	2200kg/m^3

Table 1: Geometric and material characteristics of the cantilever beam (L, l and t are the beam length, width and cross-section wall thickness, respectively, and E, ν and ρ are the concrete Young's modulus, Poisson's ratio and density, respectively).

7.2.1. Comparison of the approaches

The various methods outlined in Section 3 are first compared using the full model of the beam. Figure 8 compares the methods imposing boundary accelerations presented in Section 3.1. Since all methods are relatively accurate, every transmissibility is not plotted in Figure 8a but the relative errors are compared in Figure 8b. In this case, the formulation using relative coordinates is theoretically equivalent to the RMM; Figure 8b shows that the differences between the two

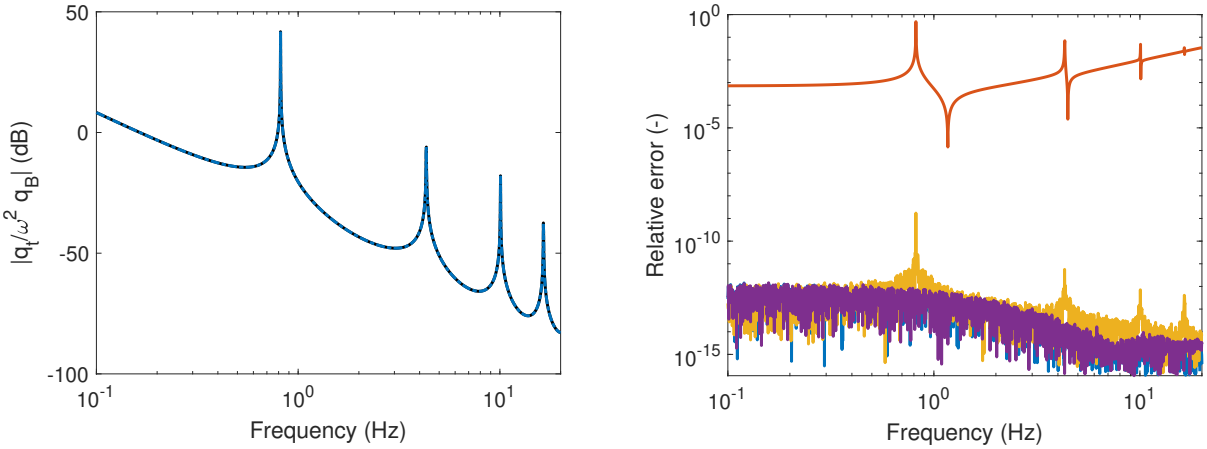

(a) (b)

Figure 8: Full model of a cantilever beam under base acceleration with the direct method (—), relative motion formulation (—), LMM (—), Lagrange multiplier method (—) and RMM (—): transmissibility (a) and relative error (b).

methods are only purely numerical and a few orders above the epsilon machine. The Lagrange multipliers method is also very accurate. The error made by this method is larger than that made by the RMM around the resonance frequencies of the structure but remains overall very small. The LMM with a penalization term $\overline{\mathbf{M}}_{BB} = 10^{10}$kg results in the largest errors among the considered methods.

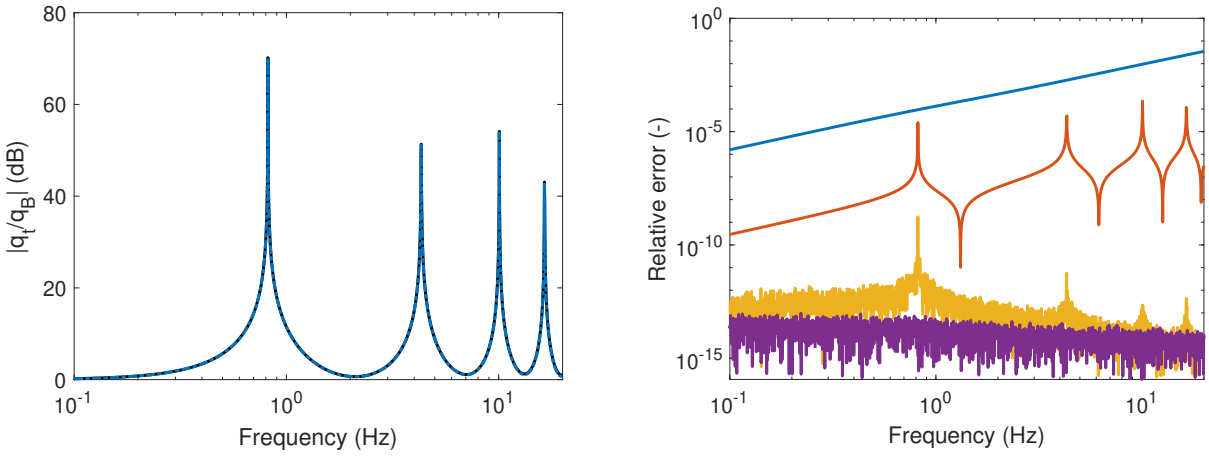

(a) (b)

Figure 9: Full model of a cantilever beam under base displacement with the direct method (—), static coupling approximation (—), LSM (—), Lagrange multiplier method (—) and RAM (—): transmissibility (a) and relative error (b).

Focusing now on methods imposing boundary displacements, Figure 9 compares the different methods discussed in Section 3.2. Since the mass matrix is not purely block diagonal, neglecting the inertial coupling term (Equation (28)) is not identical to the RAM. The former approach features the largest relative error among the methods, which is acceptably small in the low frequency

range but grows with frequency. The RAM and Lagrange multipliers method feature excellent accuracy, the latter being again slightly worse around the resonance frequencies. The LSM with a penalization term $\overline{\mathbf{K}}_{BB} = 10^{16}$N/m results in intermediate error in this case.

7.2.2. Reduced-order models

Reduced-order models of the beam are now considered with a special emphasis on Craig-Bampton models. In all cases, the transversal base and tip DoFs of the beam are retained, and five component modes are added to the model.

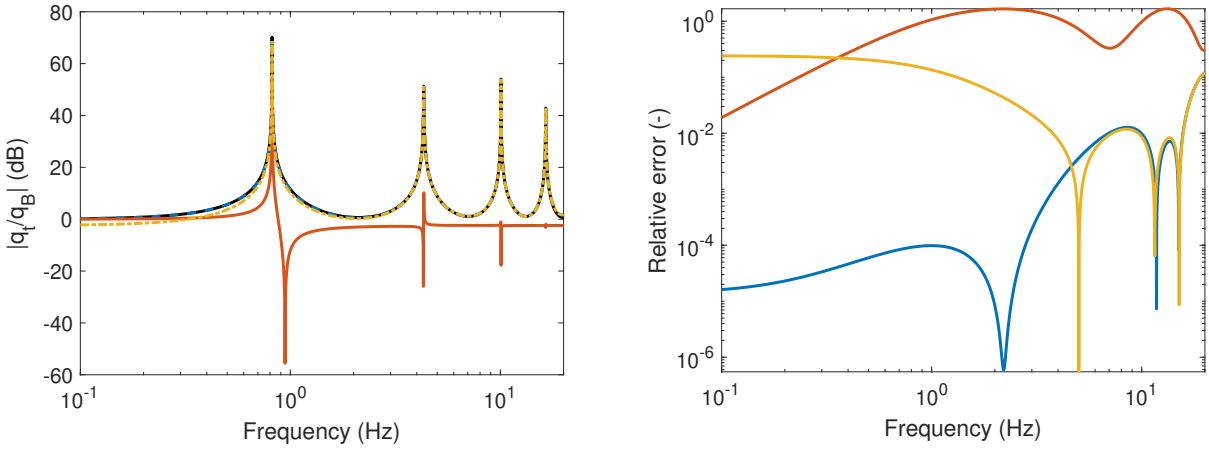

(a) (b)

Figure 10: Cantilever beam under base displacement with the direct method applied to the full model (—), direct method applied to the Craig-Bampton ROM (—), static coupling approximations with the Craig-Bampton ROM (—) and inertial coupling approximation with the Craig-Bampton ROM (—): transmissibility (a) and relative error (b).

Figure 10 investigates the case of a Craig-Bampton ROM of the beam subjected to a base displacement. The response of the full model is also given as a reference. Upon using the direct method with the ROM, an accurate reconstruction of the response of the beam is possible. However, neglecting the inertial coupling term as in Equation (28) for the ROM leads to a substantial error. The response is only exact at zero frequency, but the error rapidly increases and reaches unacceptable levels close to the first resonance, making the difference between the two transmissibilities clearly visible in Figure 10a. This was to be expected, as the interactions between the component normal modes and the retained DoFs are exclusively inertial (Equations (43) and (44)). This fact is also visually confirmed in Figure 10 by using a pure inertial coupling (i.e., neglecting the term $\mathbf{K}_{IB}\mathbf{q}_P$ in Equation (11)). In this case, a much more faithful reproduction of the transmissibility is obtained, except at low frequencies.

The foregoing discussion shows that inertial coupling terms are non-negligible when dealing with Craig-Bampton ROMs with imposed displacements. The proposed RAM is therefore expected to be particularly relevant for this case. This is confirmed in Figure 11, where the RAM applied after a Craig-Bampton reduction features a transmissibility which is as accurate as the direct method applied to the ROM. For comparison, the LSM applied to the ROM is also investigated, leading to an overall larger error than the RAM, especially around the resonance frequencies of the structure.

Finally, a MacNeal ROM is built to compare it against the Craig-Bampton one. Since one of the retained DoFs is in free conditions and the other one is fixed, neither of the ROMs is expected

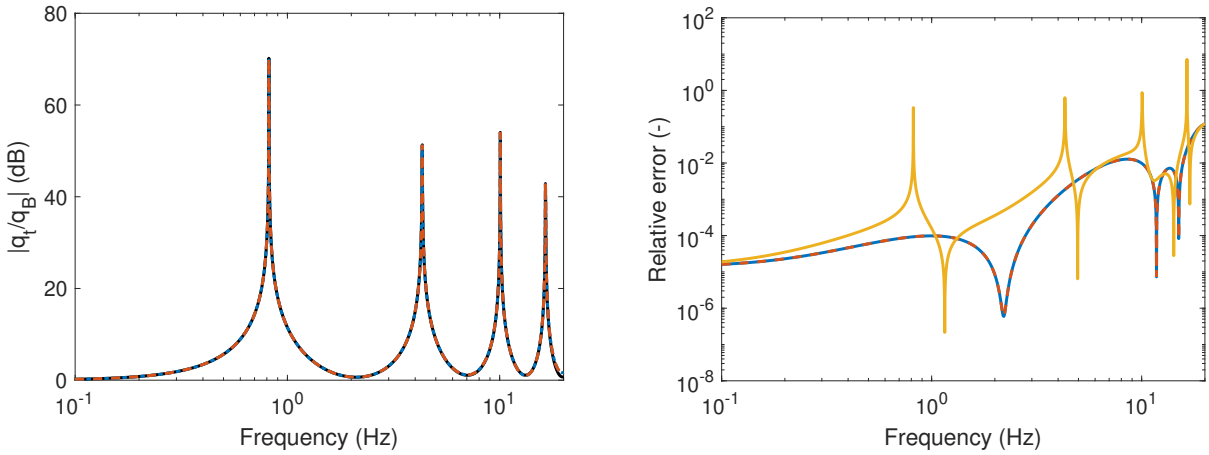

(a) (b)

Figure 11: Cantilever beam under base displacement with the direct method applied to the full model (—), direct method applied to the Craig-Bampton ROM (—), RAM applied to the Craig-Bampton ROM (—) and LSM applied to the Craig-Bampton ROM (—): transmissibility (a) and relative error (b).

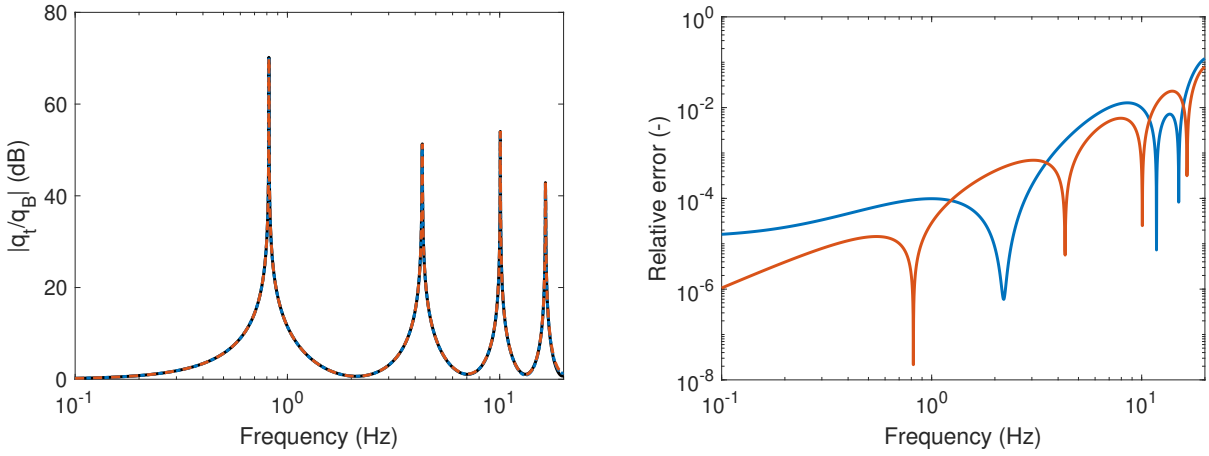

(a) (b)

Figure 12: Cantilever beam under base displacement with the direct method applied to the full model (—), RAM applied to a Craig-Bampton ROM (—) and direct method applied to a MacNeal ROM (—): transmissibility (a) and relative error (b).

to have the upper hand over the other. Figure 12 confirms this expectation. The MacNeal ROM is more accurate at low frequencies, but beyond the resonance frequency of the first mode the two ROMs feature similar errors. An advantage of the MacNeal ROM with the direct method is that it requires only the imposed displacement without need for the RAM, as discussed in Section 4.4.

7.2.3. State-space models

A final case with the cantilever beam is presented where state-space reduced models of the structure are built following the method outlined in Section 5. An acceleration is imposed to the base and Craig-Bampton ROMs are built. Two methods are used to compute the response. The first one uses relative displacements (Equation (23)) and builds a state-space model with

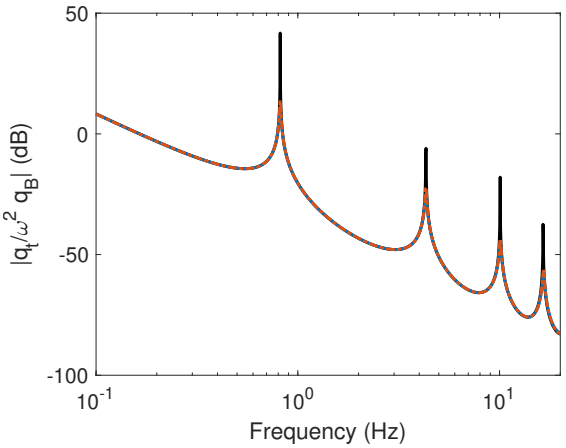

Figure 13: Transmissibility of a cantilever beam under base acceleration with the direct method applied to the full model with relative displacements (—) and Craig-Bampton ROM with relative (—) and absolute (—) displacements.

Equation (71). The absolute tip displacement is then simply deduced by adding the base motion to it. The other method uses absolute displacements and computes the state-space matrix from the reduced Craig-Bampton matrices with Equation (74). Modal damping of 1% is added to both state-space models, and both include a static correction with a feedthrough matrix. Figure 13 shows that the two methods are in perfect agreement and closely follow the reference transmissibility, except at the resonances because of the addition of modal damping.

7.3. Multi-story building

As a final example, the ten-story building model depicted in Figure 14 is considered. Each floor is a square of 10 m side discretized with 144 0.2 m-thick slab elements. The four sides and two median lines of the square are endowed with beams of square cross-section of 0.4 m side. The floors are interconnected by columns of square section of 0.6 m side, discretized with six elements between each floor. Every structural element is assumed to be made of concrete (with material characteristics given in Table 1). The full model built using the SDT [40] possesses 12 894 DoFs, thereby motivating model order reduction approaches to simulate the response in reasonable time.

A rigid support motion is imposed in the x direction, and the displacement relative to the base at one of the top corners of the structure $q_t - q_P$ is monitored to assess the structural response. In the full model, a hysteretic damping with a loss factor equal to 0.02 is used. Correspondingly, a modal damping of 1% is considered for all retained modes in the ROMs.

An imposed acceleration is considered first. Figure 15 displays the response of the structure obtained through different means. The first method uses the full model with the RMM and serves as a reference. A second method implements the RMM with the model order reduction process at the state-space model construction with 20 retained modes, as discussed in Section 5.2. A third model is built by applying the LMM to the full model with a penalization mass equal to one billion times the mass of the structure added to each support. Its Craig-Bampton ROM with 20 component normal modes is then built to evaluate the structural response. Finally, the direct method for state-space models (Equation (74)) is applied to the Craig-Bampton ROM. As shown in Figure 15, all four methods agree closely in the frequency range of the retained modes. Slight discrepancies are observable at the antiresonances due to the differences in damping models.

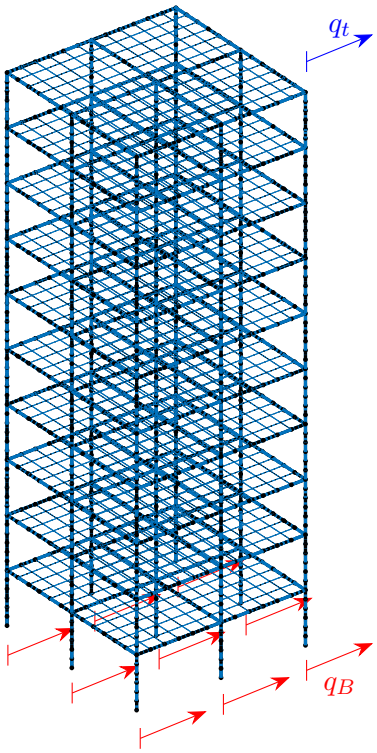

Figure 14: Ten-story building model.

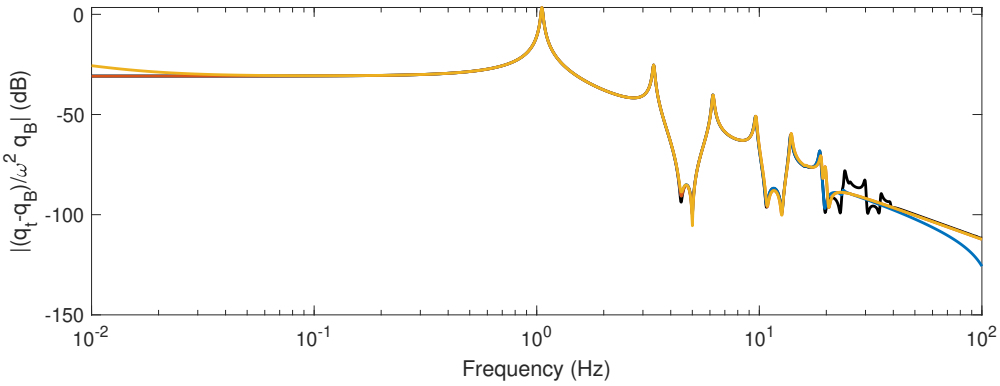

Figure 15: Transmissibility of the building model under base acceleration: RMM applied to the full model (—), state-space reduced model of the RMM (—), Craig-Bampton ROM of the LMM (—) and direct method applied to a Craig-Bampton ROM (—).

The case of an imposed base displacement is now investigated. To make the analysis comparable with methods imposing base acceleration, the transmissibility is divided by $-\omega^2$. The response of the building obtained with the RMM applied to the full building in Figure 15 is kept as a reference for comparison. Two other methods are investigated. The first one uses the LSM and reduces the state-space model using the method described in Section 5.2. The second method is the proposed RAM applied to a Craig-Bampton ROM retaining 20 component normal modes. Figure 16 compares the three results and features once again close agreement in the frequency

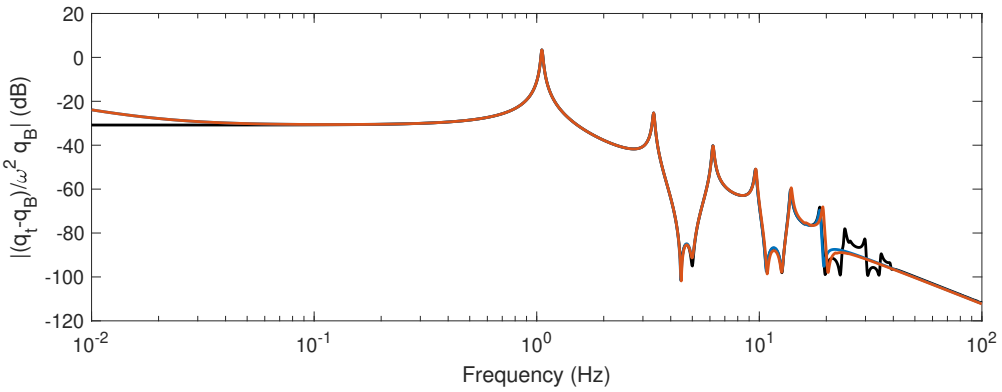

Figure 16: Transmissibility of the building model under base displacement: RMM applied to the full model with base acceleration (—), reduced state-space model of the LSM (—) and RAM applied to a Craig-Bampton ROM (—).

range of the retained modes. At low frequency, the two reduced models appear to diverge from the reference. This is due to small inaccuracies arising during the model reduction procedure, leading to a non zero static value of the relative displacement under base motion. When this static response is divided by $-\omega^2$, this error is magnified at low frequencies.

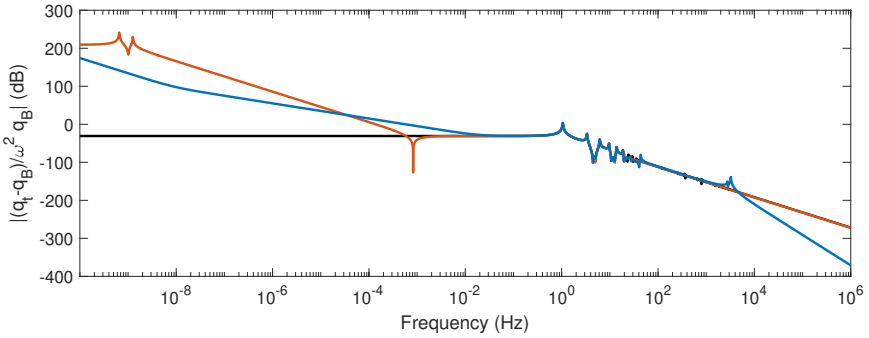

Figure 17: Transmissibility of the building model under base acceleration or displacement: RMM applied to the full model (—), Craig-Bampton ROM of the LMM (—) and reduced state-space model of the LSM with residual attachment modes (—).

Spurious modes can be introduced by some methods. As an illustration, Figure 17 depicts two such cases. In the first one, low-frequencies modes arise due to the penalization mass used in the LMM (around 1 nHz in this case). The second case is the LSM combined with a reduction including residual attachment modes (in contrast to every other reduced state-space model featuring a feedthrough term in this work). The reduction step based on a frequency criterion allows for discarding the high-frequency modes arising due to the large added penalization stiffness. However, the addition of residual attachment modes leads to spurious high-frequency modes (around 2 kHz in this case).

This example shows the ability of the presented methods to impose boundary acceleration and displacement to ROMs of large finite element models of realistic structures.

8. Conclusion

Since numerous engineering applications have to treat base-excited structural systems, this work proposed different tools to model this problem. Techniques to impose boundary acceleration and displacement were first reviewed or developed. In particular, a counterpart of the RMM for imposed displacement called RAM was introduced. Model order reduction approaches were then revisited with a specific emphasis on imposed boundary conditions. Finally, a systematic reformulation to state-space models with boundary acceleration or displacement as input was presented, including the possibility to add a static correction for improved accuracy.

These models were analyzed through three examples, and all techniques were shown to be viable with various degrees of accuracy, provided that their associated hypotheses were verified. In particular, it was shown that Craig-Bampton ROMs require caution when imposing boundary displacement. In this context, the RAM was shown to be particularly relevant.

The approaches presented herein can provide the practitioner with a toolbox to solve structural problems with time-varying imposed boundary conditions. This work could also have several potential interesting extensions. For instance, the state-space formulation readily allows for the treatment of more complex viscous damping models. The proposed approaches may also find application in active control or experimental substructuring methods. Finally, the method could be exploited to construct ROMs of piezoelectric structures [41].

Acknowledgements

Ghislain Raze is a Postdoctoral Researcher of the Fonds de la Recherche Scientifique - FNRS which is gratefully acknowledged.

References

[1] P. Léger, I. Idé, P. Paultre, Multiple-support seismic analysis of large structures, Computers & Structures 36 (6) (1990) 1153–1158. doi:10.1016/0045-7949(90)90224-P.
URL https://linkinghub.elsevier.com/retrieve/pii/004579499090224P

[2] G. Zhao, B. Ding, J. Watchi, A. Deraemaeker, C. Collette, Experimental study on active seismic isolation using interferometric inertial sensors, Mechanical Systems and Signal Processing 145 (2020) 106959. doi:10.1016/j.ymssp.2020.106959.
URL https://linkinghub.elsevier.com/retrieve/pii/S0888327020303459

[3] J.-G. Béliveau, F. Vigneron, Y. Soucy, S. Draisey, Modal parameter estimation from base excitation, Journal of Sound and Vibration 107 (3) (1986) 435–449. doi:10.1016/S0022-460X(86)80117-1.
URL https://linkinghub.elsevier.com/retrieve/pii/S0022460X86801171

[4] F. Müller, L. Woiwode, J. Gross, M. Scheel, M. Krack, Nonlinear damping quantification from phase-resonant tests under base excitation, Mechanical Systems and Signal Processing 177 (January) (2022) 109170. doi:10.1016/j.ymssp.2022.109170.
URL https://linkinghub.elsevier.com/retrieve/pii/S0888327022003272

[5] R. D. Mindlin, L. E. Goodman, Beam Vibrations With Time-Dependent Boundary Conditions, Journal of Applied Mechanics 17 (4) (1950) 377–380. doi:10.1115/1.4010161.
URL https://asmedigitalcollection.asme.org/appliedmechanics/article/17/4/377/1106510/Beam-Vibrations-With-Time-Dependent-Boundary

[6] Y. Liu, Z. Lu, Methods of enforcing earthquake base motions in seismic analysis of structures, Engineering Structures 32 (8) (2010) 2019–2033. doi:10.1016/j.engstruct.2010.02.035.
URL https://linkinghub.elsevier.com/retrieve/pii/S014102961000088X

[7] M. Géradin, D. J. Rixen, Mechanical vibrations: theory and application to structural dynamics, John Wiley & Sons, 2014.

URL https://www.wiley.com/en-us/Mechanical+Vibrations%3A+Theory+and+Application+to+Structural+Dynamics%2C+3rd+Edition-p-9781118900208

[8] R. R. Craig, M. C. C. Bampton, Coupling of substructures for dynamic analyses., AIAA Journal 6 (7) (1968) 1313–1319. doi:10.2514/3.4741.
URL https://arc.aiaa.org/doi/10.2514/3.4741

[9] A. DebChaudhury, G. D. Gazis, Response of mdof systems to multiple support seismic excitation, Journal of engineering mechanics 114 (4) (1988) 583–603. doi:10.1061/(ASCE)0733-9399(1988)114:4(583).
URL https://ascelibrary.org/doi/10.1061/%28ASCE%290733-9399%281988%29114%3A4%28583%29

[10] S. Ilanko, L. E. Monterrubio, Y. Mochida, The Rayleigh-Ritz Method for Structural Analysis, John Wiley & Sons, Inc., Hoboken, NJ, USA, 2014. doi:10.1002/9781118984444.
URL http://doi.wiley.com/10.1002/9781118984444

[11] E. A. Paraskevopoulos, C. G. Panagiotopoulos, G. D. Manolis, Imposition of time-dependent boundary conditions in FEM formulations for elastodynamics: critical assessment of penalty-type methods, Computational Mechanics 45 (2-3) (2010) 157–166. doi:10.1007/s00466-009-0428-x.
URL http://link.springer.com/10.1007/s00466-009-0428-x

[12] H. Qin, L. Li, Error Caused by Damping Formulating in Multiple Support Excitation Problems, Applied Sciences 10 (22) (2020) 8180. doi:10.3390/app10228180.
URL https://www.mdpi.com/2076-3417/10/22/8180

[13] M. Géradin, A. Cardona, Flexible multibody dynamics: a finite element approach, Wiley, 2001.
URL https://www.wiley.com/en-us/Flexible+Multibody+Dynamics%3A+A+Finite+Element+Approach-p-9780471489900

[14] J. Deng, Y. Xu, O. Guasch, N. Gao, L. Tang, Nullspace technique for imposing constraints in the Rayleigh–Ritz method, Journal of Sound and Vibration 527 (February) (2022) 116812. doi:10.1016/j.jsv.2022.116812.
URL https://linkinghub.elsevier.com/retrieve/pii/S0022460X22000633

[15] R. H. MacNeal, A hybrid method of component mode synthesis, Computers & Structures 1 (4) (1971) 581–601. doi:10.1016/0045-7949(71)90031-9.
URL https://linkinghub.elsevier.com/retrieve/pii/0045794971900319

[16] S. Rubin, Improved Component-Mode Representation for Structural Dynamic Analysis, AIAA Journal 13 (8) (1975) 995–1006. doi:10.2514/3.60497.
URL https://arc.aiaa.org/doi/10.2514/3.60497

[17] D. J. Rixen, A dual Craig–Bampton method for dynamic substructuring, Journal of Computational and Applied Mathematics 168 (1-2) (2004) 383–391. doi:10.1016/j.cam.2003.12.014.
URL https://linkinghub.elsevier.com/retrieve/pii/S0377042703010045

[18] D. de Klerk, D. J. Rixen, S. N. Voormeeren, General Framework for Dynamic Substructuring: History, Review and Classification of Techniques, AIAA Journal 46 (5) (2008) 1169–1181. doi:10.2514/1.33274.
URL https://arc.aiaa.org/doi/10.2514/1.33274

[19] B. Besselink, U. Tabak, A. Lutowska, N. van de Wouw, H. Nijmeijer, D. Rixen, M. Hochstenbach, W. Schilders, A comparison of model reduction techniques from structural dynamics, numerical mathematics and systems and control, Journal of Sound and Vibration 332 (19) (2013) 4403–4422. doi:10.1016/j.jsv.2013.03.025.
URL https://linkinghub.elsevier.com/retrieve/pii/S0022460X1300285X

[20] D. Krattiger, L. Wu, M. Zacharczuk, M. Buck, R. J. Kuether, M. S. Allen, P. Tiso, M. R. Brake, Interface reduction for Hurty/Craig-Bampton substructured models: Review and improvements, Mechanical Systems and Signal Processing 114 (2019) 579–603. doi:10.1016/j.ymssp.2018.05.031.
URL https://linkinghub.elsevier.com/retrieve/pii/S088832701830284X

[21] E. J. Kuhar, C. V. Stahle, Dynamic Transformation Method for Modal Synthesis, AIAA Journal 12 (5) (1974) 672–678. doi:10.2514/3.49318.
URL https://arc.aiaa.org/doi/10.2514/3.49318

[22] Q. Aumann, E. Deckers, S. Jonckheere, W. Desmet, G. Müller, Automatic model order reduction for systems with frequency-dependent material properties, Computer Methods in Applied Mechanics and Engineering 397 (2022) 115076. doi:10.1016/j.cma.2022.115076.
URL https://linkinghub.elsevier.com/retrieve/pii/S004578252200281X

[23] Gene F. Franklin, J. David Powell, Abbas Emami-Naeini, Feedback Control of Dynamic Systems, Pearson London, 2015.
URL https://www.pearson.com/uk/educators/higher-education-educators/program/Franklin-Feedback-Control-of-Dynamic-Systems-Global-Edition-8th-Edition/PGM2639960.html

[24] E. Balmès, New Results on the Identification of Normal Modes from Experimental Complex Modes, Mechanical

Systems and Signal Processing 11 (2) (1997) 229–243. doi:10.1006/mssp.1996.0058.
URL https://linkinghub.elsevier.com/retrieve/pii/S0888327096900588

[25] F. M. Gruber, D. J. Rixen, Dual Craig-Bampton component mode synthesis method for model order reduction of nonclassically damped linear systems, Mechanical Systems and Signal Processing 111 (2018) 678–698. doi:10.1016/j.ymssp.2018.04.019.
URL https://linkinghub.elsevier.com/retrieve/pii/S0888327018302218

[26] T. McKelvey, H. Akcay, L. Ljung, Subspace-based multivariable system identification from frequency response data, IEEE Transactions on Automatic Control 41 (7) (1996) 960–979. doi:10.1109/9.508900.
URL http://ieeexplore.ieee.org/document/508900/

[27] K. F. Alvin, K. C. Park, Second-order structural identification procedure via state-space-based system identification, AIAA Journal 32 (2) (1994) 397–406. doi:10.2514/3.11997.
URL https://arc.aiaa.org/doi/10.2514/3.11997

[28] M. De Angelis, H. Lus¸, R. Betti, R. W. Longman, Extracting Physical Parameters of Mechanical Models From Identified State-Space Representations, Journal of Applied Mechanics 69 (5) (2002) 617–625. doi:10.1115/1.1483836.
URL https://asmedigitalcollection.asme.org/appliedmechanics/article/69/5/617/445202/Extracting-Physical-Parameters-of-Mechanical

[29] H. Luş, M. De Angelis, R. Betti, R. W. Longman, Constructing Second-Order Models of Mechanical Systems from Identified State Space Realizations. Part I: Theoretical Discussions, Journal of Engineering Mechanics 129 (5) (2003) 477–488. doi:10.1061/(ASCE)0733-9399(2003)129:5(477).
URL http://ascelibrary.org/doi/10.1061/%28ASCE%290733-9399%282003%29129%3A5%28477%29

[30] M. Gibanica, T. J. Abrahamsson, Identification of physically realistic state-space models for accurate component synthesis, Mechanical Systems and Signal Processing 145 (2020) 106906. doi:10.1016/j.ymssp.2020.106906.
URL https://doi.org/10.1016/j.ymssp.2020.106906

[31] M. Gibanica, T. J. Abrahamsson, T. McKelvey, State-space system identification with physically motivated residual states and throughput rank constraint, Mechanical Systems and Signal Processing 142 (2020) 106579. doi:10.1016/j.ymssp.2019.106579.
URL https://doi.org/10.1016/j.ymssp.2019.106579

[32] P. Sjövall, T. Abrahamsson, Component system identification and state-space model synthesis, Mechanical Systems and Signal Processing 21 (7) (2007) 2697–2714. doi:10.1016/j.ymssp.2007.03.002.
URL https://linkinghub.elsevier.com/retrieve/pii/S088832700700043X

[33] M. Scheel, M. Gibanica, A. Nord, State-Space Dynamic Substructuring with the Transmission Simulator Method, Experimental Techniques 43 (3) (2019) 325–340. doi:10.1007/s40799-019-00317-z.
URL http://link.springer.com/10.1007/s40799-019-00317-z

[34] D. S. Bernstein, Matrix mathematics, in: Matrix Mathematics, Princeton university press, 2009.
URL https://doi.org/10.1515/9781400833344

[35] T. Ghosh, Improved method of generating control system model using modal synthesis, in: Modeling and Simulation Technologies Conference, American Institute of Aeronautics and Astronautics, Reston, Virigina, 1997, pp. 231–239. doi:10.2514/6.1997-3673.
URL https://arc.aiaa.org/doi/10.2514/6.1997-3673

[36] C. Monjaraz Tec, J. Gross, M. Krack, A massless boundary component mode synthesis method for elastodynamic contact problems, Computers & Structures 260 (2022) 106698. doi:10.1016/j.compstruc.2021.106698.
URL https://linkinghub.elsevier.com/retrieve/pii/S0045794921002200

[37] R. Craig, Jr., Coupling of substructures for dynamic analyses - An overview, in: 41st Struct. Struct. Dyn. Mater. Conf. Exhib., American Institute of Aeronautics and Astronautics, Reston, Virigina, 2000. doi:10.2514/6.2000-1573.
URL https://arc.aiaa.org/doi/10.2514/6.2000-1573

[38] M. De Angelis, M. Imbimbo, A Procedure to Identify the Modal and Physical Parameters of a Classically Damped System under Seismic Motions, Advances in Acoustics and Vibration 2012 (2012) 1–11. doi:10.1155/2012/975125.
URL https://www.hindawi.com/journals/aav/2012/975125/

[39] J. C. O'Callahan, System equivalent reduction expansion process, in: Proceedings of the 7th International Modal Analysis Conference, 1989.

[40] E. Balmes, G. Vermot des Roches, G. Martin, J.-P. Bianchi, Structural Dynamics Toolbox & FEMLink (feb 2019).
URL https://www.sdtools.com/help/sdt.pdf

[41] G. Raze, J. Dietrich, A. Paknejad, B. Lossouarn, G. Zhao, A. Deraemaeker, C. Collette, G. Kerschen, Passive control of a periodic structure using a network of periodically-coupled piezoelectric shunt circuits, in: W. Desmet, B. Pluymers, D. Moens, S. Vandemaele (Eds.), Proceedings of ISMA 2020-International Conference on Noise and Vibration Engineering and USD 2020-International Conference on Uncertainty in Structural Dynamics, KU Leuven, Leuven, 2020, pp. 145–160.
URL https://orbi.uliege.be/handle/2268/252957